Journal of Geochemical Exploration 138 (2014) 33–49

Contents lists available at ScienceDirect

Journal of Geochemical Exploration

journal homepage: www.elsevier.com/locate/jgeoexp

Evaluation of trace elements and identification of pollution sources in particle size fractions of soil from iron ore areas along the Chao River

Qin Fei [a], Ji Hongbing [a,b,*], Li Qian [a], Guo Xinyue [a], Tang Lei [a,c], Feng Jinguo [c]

[a] Civil and Environmental and Engineering School, University of Science and Technology Beijing, Beijing100083, China
[b] State Key Laboratory of Environmental Geochemistry, Institute of Geochemistry, Chinese Academy of Sciences, Guiyang 550002, China
[c] Beijing Geo-engineering Design and Research Institute, Beijing 101500, China

ARTICLE INFO

Article history:
Received 12 August 2013
Accepted 12 December 2013
Available online 21 December 2013

Keywords:
Soil
Size fraction
Cluster analysis
Principal component analysis
Enrichment factor
Potential ecological hazard index

ABSTRACT

This study examines the distributions and potential environmental risk posed by trace elements in various particle size fractions. Element concentrations in soil samples from the study site exceed those of background levels in Beijing, except for Pb and As. The element concentrations generally increased with the decrease of particle size. Both correlation and linear analyses showed positive correlations between element concentrations and organic matter content. The PCA and CA analyses showed that: (1) Cu, Co, Zn, Cd, and V originated from mixed sources; (2) Be, Pb and As came from natural sources and were mainly affected by weathering and erosion of parent rock material; (3) Cr, Ni, and Ba resulted from fine particle pollution; and (4) Hg originated from anthropogenic sources, mainly driven by mining, beneficiation, smelting and acid mine drainage. The Enrichment Factor and Potential ecological harm-indices suggested that the enrichment degree of RI and E_r^i, increased with the decrease of the particle size, especially for Hg and Cd. This conclusion provides a scientific basis for the prevention of environmental pollution from mining and the protection of the Miyun Reservoir in Beijing. It also provides reference for the further study of trace elements in various particle size fractions internationally.

1. Introduction

Soil is one of the natural resources on which the human beings rely, and is a place for interaction of environmental elements (Chen et al., 2003; Zhao and Tang, 2011). In recent years, public attention has been increasingly focused on soil contamination as well as its effect on human beings and other creatures. Among the various pollutants, trace elements are particularly important. Because they contaminate soils and plants and enter food chains, posing health problems to human beings. However, there is considerable variation in the level of these contaminants in soil, depending on their natural and anthropogenic sources. The natural sources are primarily rocks (Tuchschmid et al., 1995), minerals, and atmospheric deposition (Nriagu and Pacyna, 1988; Oliva and Espinosa, 2007), while anthropogenic sources mainly include direct or indirect emissions of trace elements from human activities, such as, mining, smelting(Adriano, 1986; Al et al., 1997; Jordan, 2009; Navarroa et al., 2008), the burning of fossil fuels, waste incineration and disposal, sewage irrigation, the use of leaded gasoline and motor traffic, production and extensive use of chemical fertilizers and pesticide, daily activities, aerosolized trace elements, etc. (Dong et al., 1984; Lagerwerff and Specht, 1970; Purve, 1977; Rybicka, 1987). Trace elements in soil cannot be degraded by microorganisms (Harte et al., 1991; Nuremberg, 1984), but they can accumulate and be absorbed by crops (Zhong et al., 2009), enter the human body through direct contact or the food chain (Government of Canada, 2001; Lin et al., 1998; Wenzel and Jockwer, 1999) and harm human health (Agbozu et al., 2007; Luo et al., 2012a).

Soil particle size is an important factor in determining the mobility of trace elements. Since the 1980s, international scholars have carried out research on the distribution of particle size of trace elements in surface soil (Ahmed and Ishiga, 2006; Viklander, 1998). The concentration (Förstner and Wittmann, 1979), migration, and transformation of trace element pollutants are all closely related to the particle size, because, fine particulate matter acts as a carrier for trace elements in soils, bringing potential risks to the environment and human health (Dominici et al., 2006; Vallejo et al., 2006). The concentrations of trace elements in soils increase with the decrease of particle size, because, fine particles have greater specific surface area, a negative charge, high clay content and high organic content. (Baek et al., 1997; Barberis et al., 1992; Charlesworth and Lees, 1999). The different types of clay minerals, particularly montmorillonite, kaolinite and illite, also adsorb trace elements (Brady, 1985). Research and evaluation on the activity and potential environmental risk resulted from trace elements in different size fraction components can further strengthen our understanding on the transfer and transformation of trace elements, and may provide strategies to repair and control the pollution. However Chinese scholars mainly focus on the study of characteristics and spatial distribution of

* Corresponding author at: State Key Laboratory of Environmental Geochemistry, Institute of Geochemistry, Chinese Academy of Sciences, Guiyang 550002, China. Tel./fax: +86 10 62332747.
E-mail address: hongbing_ji@163.com (H. Ji).

0375-6742/$ – see front matter © 2013 Elsevier B.V. All rights reserved.
http://dx.doi.org/10.1016/j.gexplo.2013.12.005

trace elements in the surface bulk soil sample (Li et al., 2008; Qu et al., 2008; Wang et al., 2003). Analyses of the effect of grain size on trace element pollution and potential risk assessments have only been carried out by a few researchers (Zheng et al., 2010).

The primary objective of the study was to examine iron ore area along the banks of the Chao River in Miyun. We gathered soil samples which are typical of iron ore mining, and established the source and distribution of trace elements in the region through multivariate statistical analysis such as clustering analysis and factor analysis. Furthermore, we aimed to determine the level of trace element pollution by applying an enrichment factor and calculating a potential ecological damage index, and to reveal the relationship between the concentrations of trace elements and particle size distribution. This work will provide a scientific basis for preventing and controlling trace element contamination.

2. Materials and methods

2.1. Study area

The study area centered on iron ore deposit located east of Beijing near the Miyun Reservoir. The Miyun Reservoir (40°23′ N, 116°50′ E) was built in 1960 and has a surface area of 188 km^2, with a catchment area of approximately 15,788 km^2. It is the largest reservoir in northern China and consists of eastern and western reservoirs as well as a closed independent water body referred to as the inner lake. Two main rivers, the Chao and the Bai, flow into the Miyun Reservoir. Surface runoff roughly mirrors precipitation, with large interannual fluctuations and an uneven distribution throughout the year. The Miyun Reservoir has been used as drinking water storage for Beijing since 1997. The water quality of Miyun Reservoir directly affects the health and safety of the residents of Beijing.

On the eastern side of the reservoir, there are rich iron ore resources. Frequent mining activities produce dust, mill tailings and large quantities of acidic drainage from the oxides generated by mining, beneficiation and smelting. Each of these influences the soil and water of the area. This study took place in the iron ore area along the banks of the Chao River. Soil samples were gathered from typical iron ore mining areas (Fig. 1).

2.2. Sampling and analytical methods

Thirty soil samples were collected from separate locations in an area of iron ore along the bank of Chao River according to the sampling grid shown in Fig. 1. Each soil sample (or bulk sample) was taken from the surface (0–15 cm) using a soil spade and stored in plastic bags. We took precautions to ensure that, the samples were not affected by metal equipments or tools. At each sampling site, composite samples were obtained by mixing subsamples from four points taken from each corner of a 1 m^2 square. We used surface soil because trace element additions to soils occurred mostly in top-soil. Soil samples were stored in polyethylene bags and kept at 4 °C prior to sample preparation and analyses. Samples were air-dried, gently crushed and sieved at 2 mm with a plastic sieve and then ground, homogenized with an agate mortar and sieved again through a 200 mesh sieve for laboratory analyses.

In according to the method that choosing the first and third in singular line of the grid, selecting the fourth and sixth in dual line, we selected 10 samples. Then according to the principle of clay (<2 μm), fine powder sand grains (2–5 μm), coarse powder sand grains (5–50 μm) and sand (>50 μm), the selected 10 samples were partitioned into seven size fractions: <2 μm, 2–5 μm, 5–10 μm, 10–50 μm, 50–74 μm, 74–165 μm and 165–350 μm. To separate them, the air-dried soil samples were passed, through a 40 mesh (350 μm), 100 mesh (165 μm)

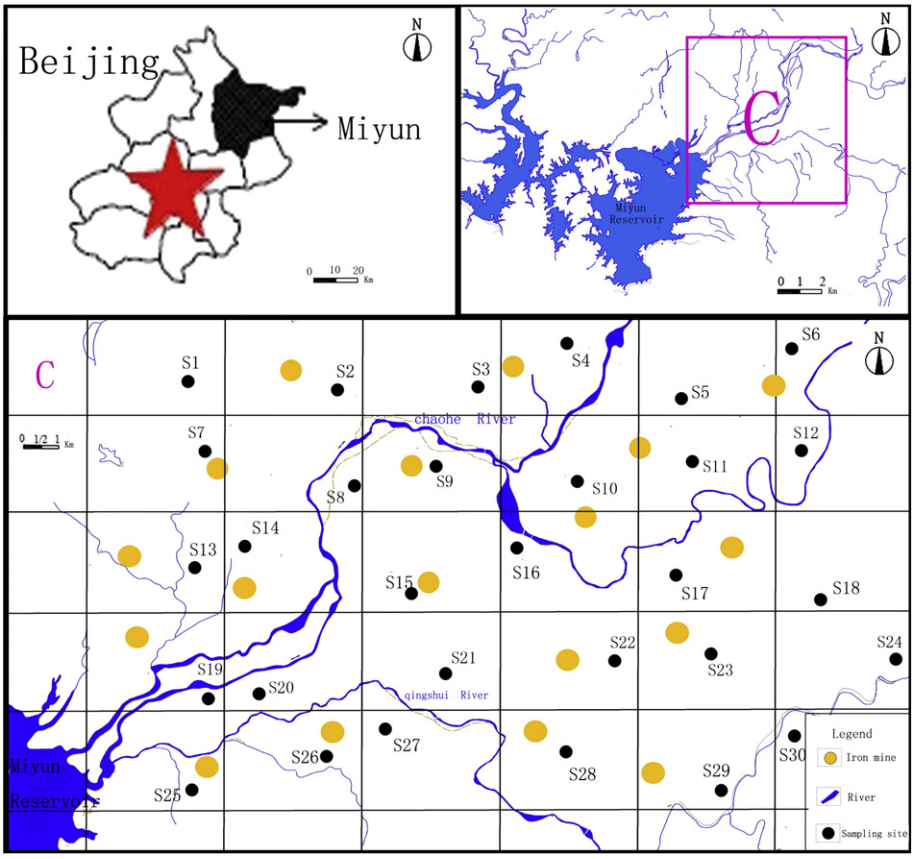

Fig. 1. Schematic map of the study area and sampling points.

and 200 mesh sieve (74 μm). Then, 100 g of the soil from the 200 mesh sieve was dispersed with Na-hexametaphosphate for 16 h by horizontal shaking. The <2 μm fraction was separated by centrifugation, and the remaining fractions by repeated sedimentation and decanting. After separation, all the fractions were dried and weighted.

The soil samples were analyzed for their chemical and physical properties. The pH was determined potentiometrically in a soil-$CaCl_2$ (0.01 M) suspension (ratio soil:solution 1:5, ISO 10390). The total organic carbon content was measured with a TOC analyzer made by Germany Elementar Company.

For bulk soil samples and size fractions the concentrations of Be, Ba, V, Co, Cr, Cu, Pb, Zn, Cd and Ni were determined by inductively coupled plasma mass spectrometry (ICP-MS). A sample (0.10 g) was placed into a Teflon beaker, and 1.5 ml HF, 1 ml HNO_3 and 2 ml H_2O_2 were then added. The beaker was placed on a hot plate (~140 °C) for 48 h until the sample was completely dissolved and vaporized to dryness. Afterwards, 1 ml HNO_3 was added with an appropriate amount of ultrapure water, and the mixture was heated so that the salts dissolved completely. The resulting solution was placed into a 50 ml plastic bottle and measured against the internal standard. All the analyses were conducted alongside standards. The above analyses and measurements were all performed at the Analysis Research Center of Nuclear Industry Geological Institute in Beijing. Detection limit ranges of Be, V, Cr, Zn and Ni are the same, which is 0.1–1 ppt, detection limit ranges of Ba, Co, Cu, Pb and Cd are <0.1 ppt.

For bulk soil samples and size fractions the concentrations of As, and Hg were determined by atomic fluorescence spectroscopy (AFS). A sample (0.10 g) was placed in a colorimetric tube, and was then digested with aqua regia (HCl/HNO_3, 3:1 v/v) in a 95 °C water bath for 2 h with 4 oscillations. Afterwards, ultrapure water was added to bring the solution to 50 ml. A 25 ml subsample was collected. After 5 ml HCL (1.19 g · ml^{-1}) and 5 ml thiourea (50 g · L^{-1}) were added, the solution was again brought to a constant volume of 50 ml for 30 min before analysis. Accuracy was checked against a certified reference material (GBW07403). Detection limit range of As is <0.01 μg/L, detection limit range of Hg is <0.001 μg/L.

X-ray diffraction (XRD) was used to determine the mineral composition of bulk and fractionated samples. The six soil samples in the study were ground in an agate mortar and analyzed using X-ray diffraction (XRD). The semiquantitative calculation of mineral composition was based on the *K* value method (Schultz, 1964). We used the Dmax/2200 model made in Japan as the experimental apparatus, using the instrument standard CuKα target, 40 kV, 20 mA, the scanning scope for 2–60°, the scanning step length for 0.04°, and a scanning speed for 10°/min. Samples were randomly mounted on glass petrographic slides and then analyzed in air-dried, ethylene glycol at 300 and 550 °C for identification prior to XRD analysis (Ji et al., 2004).

2.3. Multivariate statistical method

Multivariate statistical methods offer powerful tools for monitoring soil properties. Recently, such methods have been widely applied to investigate trace element concentration, accumulation and distribution in soils, as documented by several studies (Lin et al., 2002; Qishlaqi and Moore, 2007; Salman and Abu Rukah, 1999) that multivariate statistical methods are used to study the behavior, distribution and interrelationship of trace elements in soils.

Principal component analyses (PCAs) can reduce the complexity of large-scale data sets and are broadly used in environmental impact studies (Perona et al., 1999) to elucidate relations among variables by identifying common underlying processes (Farnham et al., 2003; Webster and Oliver, 1990). The number of significant principal components is selected on the basis of the Kaiser criterion of eigenvalues higher than 1 (Kaiser, 1960) and a total explained variance is equal to or higher than 85%.

Cluster analysis (CA) is often coupled with PCA to check results and group the individual parameters and variables (Facchinelli et al., 2001). Cluster analysis (CA) is a group of multivariate technique, which allows the assembly of objects based on the characteristics. CA classifies objects, so that each object is similar to the others in the cluster with respect to a predetermined selection criterion. Hierarchical agglomerative clustering is the most common approach, which provides intuitive similarity relationships between any one variable and the entire data set and is typically illustrated by a dendrogram (tree diagram). The dendrogram provides a visual summary of the clustering processes, presenting a picture of the groups and their proximity with a dramatic reduction in dimensionality of the original data (Shrestha and Kazama 2007).

2.4. Accumulation factor and enrichment factor

Sheppard and Evenden proposed using a factor to calculate the relative accumulation of trace elements in the fine fractions in 1992. The equation (Ajmone-Marsan et al., 2008) can be represented as:

$$AF = C_{fraction}/C_{bulk}$$

where $C_{fraction}$ and C_{bulk} are concentrations of trace element (mg · kg^{-1}) in a given particle size fraction and in the bulk sample, respectively.

The enrichment factor is the parameter that evaluates on the impact of human activities on the concentrations of trace elements in soils (Ansari et al., 2000; Lee et al., 1994; Middleton and Grant, 1990). In order to reduce human impacts during the process of sampling and sample preparation and to ensure comparability and equivalence among the various indicators with the reference standard, the elements in the test sample were normalized (Li et al., 2006; Teng et al., 2002). The value of the enrichment factor was calculated by a modified formula (Buat-Menard and Chesselet, 1979; Li, 1981; Sutherland, 2000):

$$EF = \left(C_n/C_{ref(sample)}\right)/\left(B_n/B_{ref(background)}\right)$$

where $C_{n(sample)}$ and $B_{n(background)}$ are concentrations of a trace element (mg · kg^{-1}) in the test and reference areas, respectively and $C_{ref(sample)}$ and $B_{ref(background)}$ are concentrations of the reference element (mg · kg^{-1}) in the test and reference areas, respectively.

2.5. Potential ecological hazard index

The potential ecological hazard index suggested by the Swedish scientist Hankinson reflects not only the effects of a single trace element in a particular environment but also the compound influence of many trace elements. It uses quantitative methods to parse the degree of potential ecological hazard degree and is widely used in pollution assessments of trace elements in soils and sediments. The calculation includes four steps (Hakanson, 1980):

1) The contamination factor of a single trace element, or C_r^i is

$$C_r^i = C_{surface}^i/C_n^i$$

where $C_{surface}^i$ is the measured concentration of trace elements in the soil (or sediment); and $C_n^i$is the reference value. The reference value is set as the highest background value of trace elements in sediments in modern preindustrial times as suggested by Hakanson, although some scholars use national soil environmental standard values as the reference.

2) The toxic response factor of trace elements, T_r^i is used to reflect the response of trace elements in water, sedimentary and biological phases. A standardized trace element toxic response coefficient is taken as the assessment standard as suggested by Hakanson. The toxic response coefficients are Be = Ba = Zn = 1 < V = Cr =

$2 < Cu = Ni = Co = Pb = 5 < As = 10 < Cd = 30 < Hg = 40$ (Y.N. Xu et al., 2008; Z.Q. Xu et al., 2008);

3) The potential ecological risk index, E_r^ican then be calculated for each trace element:

$$E_r^i = T_r^i \times C_r^i$$

4) The potential ecological risk index of various trace elements, or RI can be divided in to five levels such that the potential ecological harm is.

$$RI = \sum_{i=1}^{n} E_r^i$$

3. Results

3.1. Soil physical and chemical properties

The pH and organic matter (OM) content of bulk soils in an area of iron ore along the Chao River in the upper reaches of the Miyun Reservoir are shown in Table 1. The soil pH is mainly acidic, ranging from pH 4.88 to 6.90. The most acidic was sample S14, from the topsoil of an iron mine near Dacao Village. This value might reflect the dust and tailings generated by smelting and the acidic mine drainage produced by the iron ore oxide. The organic matter content in the study area ranged from 0.23% to 5.16%. The highest was found in S29, which was surface soil from cropland near Yingfang. It may result from organic fertilizer. These conclusions are consistent with previous results (Gao et al., 2012; Huang et al., 2012).

3.2. Soil mineral properties

The soil minerals in the bulk soils used in this study were very similar and consisted of quartz, feldspar, montmorillonite, dolomite, and calcite with minor amounts of illite, hornblende, kaolinite, and iron ore (Fig. 2). Semi-quantitative estimates of dominant minerals were as follows: quartz (42.49%–69.62%) > feldspar (42.49%–38.62%) > montmorillonite (3.45%–21.65%) > dolomite (4.62% 9.13%). These minerals are likely to adsorb trace elements and move them to the fine particulate matter; for example, Ni, Cd, Zn, Pb, As and Cu from soil are highly enriched in clay minerals (Matini et al., 2011; Schulthess and Huang, 1990; Usman et al., 2004). Feldspar is usually the most widely distributed mineral in the crust and accounts for approximately 50% of the mass of the earth's crust. Previous results (Li et al., 2007) show that feldspar minerals at temperatures ranging from low to high can undergo ion exchange and display the pore structure that allows surface adsorption of minerals via, channel filters, etc.

3.3. Characteristics of soil elements in bulk and particle size fractions

Be, Ba, V, Cr, Co, Ni, Cu, Zn, Cd, Pb, As and Hg were analyzed, and their concentrations are shown in Table 1. In more than 24 of the total 30

Table 1
Contents of trace elements and organic carbon, and pH value in soils of the study area.

Serial number	Contents of heavy metals/(mg · kg^{-1})												pH	OM (%)
	Be	Ba	V	Cr	Co	Ni	Cu	Zn	Cd	Pb	As	Hg		
S1	1.77	655	110	121	19	49.4	49.2	130	0.186	25.3	7.142	0.235	6.54	2.43
S2	1.56	707	115	126	17.7	43.9	41.2	110	0.224	22.2	4.722	0.252	6.31	1.76
S3	1.33	723	121	185	19.9	49.8	80.9	137	0.154	15.2	3.655	0.211	5.88	0.86
S4	1.21	487	50.6	104	22.8	72.3	114	159	0.212	7.86	4.209	0.543	6.46	0.50
S5	1.68	978	69.9	94.2	11.6	31.1	26.5	101	0.154	18.9	5.525	0.329	5.54	1.03
S6	2.11	608	98.5	73.3	15.5	35.5	35.9	103	0.129	25.3	9.405	0.310	6.46	1.55
S7	1.72	659	91.7	89.1	15.2	36.5	62.9	129	0.208	21.5	7.993	0.275	5.36	1.12
S8	1.86	619	87.4	71.8	13.6	31.1	32.9	98.8	0.143	22.9	7.189	0.339	5.35	1.37
S9	1.32	774	116	233	22.6	72.6	53.5	108	0.133	14.9	2.722	0.299	5.50	0.67
S10	1.81	624	89.2	75.2	13.5	31.8	31.9	99.2	0.143	22.2	7.880	0.331	5.57	1.32
S11	1.98	1044	139	110	21	41.2	39.8	126	0.113	20.6	4.871	0.277	6.62	0.70
S12	2.04	717	86.3	62.9	12.9	26.4	29.6	97.9	0.127	23.6	6.716	0.469	6.62	1.20
S13	1.91	646	104	85.8	15.7	37.6	38.3	102	0.116	23.4	7.472	0.295	6.34	1.22
S14	1.67	705	114	153	20.1	56.3	50.4	109	0.162	19.3	6.862	0.310	4.88	0.83
S15	1.01	771	117	281	25.2	99.5	66.5	110	0.136	10.4	1.876	0.331	6.05	0.23
S16	1.65	704	117	106	15.2	33.8	38.5	94.9	0.124	18.2	4.687	0.375	6.42	1.53
S17	1.94	760	69.3	51.9	9.98	21.6	24.5	99.3	0.123	22.2	6.018	0.252	6.69	1.29
S18	1.93	971	131	88.6	19.1	33.4	38.3	138	0.219	23.3	5.322	0.381	6.66	1.78
S19	1.95	767	112	109	18	44.9	45.2	122	0.165	28.5	7.156	0.333	6.59	2.15
S20	1.38	863	141	269	27.7	95.8	65.3	148	0.231	20.4	3.714	0.806	6.78	2.49
S21	2.04	729	115	128	18.6	47.6	46.1	108	0.156	20.9	6.609	0.421	6.59	1.79
S22	1.49	795	158	129	26.2	47.8	69.6	124	0.162	18	4.091	0.490	5.94	1.57
S23	1.92	800	69.1	55.1	10.5	22.4	24.5	92.8	0.116	23.6	5.672	0.324	5.86	1.98
S24	1.54	811	69.5	86.1	14.3	37.4	45.3	111	0.193	17.7	4.675	0.454	6.78	2.48
S25	2	966	101	84.1	15.3	29.8	39.4	109	0.181	25.8	9.396	0.396	6.26	2.24
S26	1.49	705	115	148	21.2	61.9	41.6	115	0.173	16.2	5.380	0.362	6.37	0.82
S27	1.69	1060	185	141	21.7	33.7	59.1	110	0.153	16.2	4.022	0.390	6.67	1.31
S28	1.52	804	106	151	17.2	45.6	39.9	92.8	0.159	17.1	6.603	0.382	6.66	1.30
S29	1.69	600	76.7	56.8	11.5	28.5	31.3	103	0.175	24.2	10.792	0.358	6.90	5.16
S30	1.92	683	86	63.6	13	28.8	33.1	99	0.179	22.8	9.841	0.303	6.80	2.83
Minimum	1.01	487	50.6	51.9	9.98	21.6	24.5	92.8	0.110	7.86	1.88	0.210	4.88	0.23
Maximum	2.11	1060	185	281	27.7	99.5	114	159	0.230	28.5	10.79	0.810	6.90	5.16
Median	1.69	723	106	104	17.2	37.4	39.9	109	0.160	20.9	5.67	0.330	6.42	1.32
Mean	1.70	757.8	105.4	118	17.5	44.3	46.5	113	0.160	20.3	6.07	0.360	6.25	1.58
Background in Beijing	1.35	522	77.4	66.7	15.0	28.2	23.1	97.2	0.0534	24.7	9.4	0.0576		
Mean/background in Beijing	1.3	1.5	1.4	1.8	1.2	1.6	2	1.2	3	0.8	0.65	6.3		
SD	0.28	136.6	28.6	59.0	4.7	19.4	19.0	16.8	0.33	4.55	2.14	0.11	0.53	0.93
Skewness	−0.66	0.65	0.57	1.48	0.37	1.55	1.78	1.12	0.48	−0.85	0.30	2.23	−0.98	1.98
Kurtosis	−0.13	0.21	0.96	1.96	−0.54	2.24	4.35	0.74	−0.64	0.94	−0.25	7.39	0.01	6.54

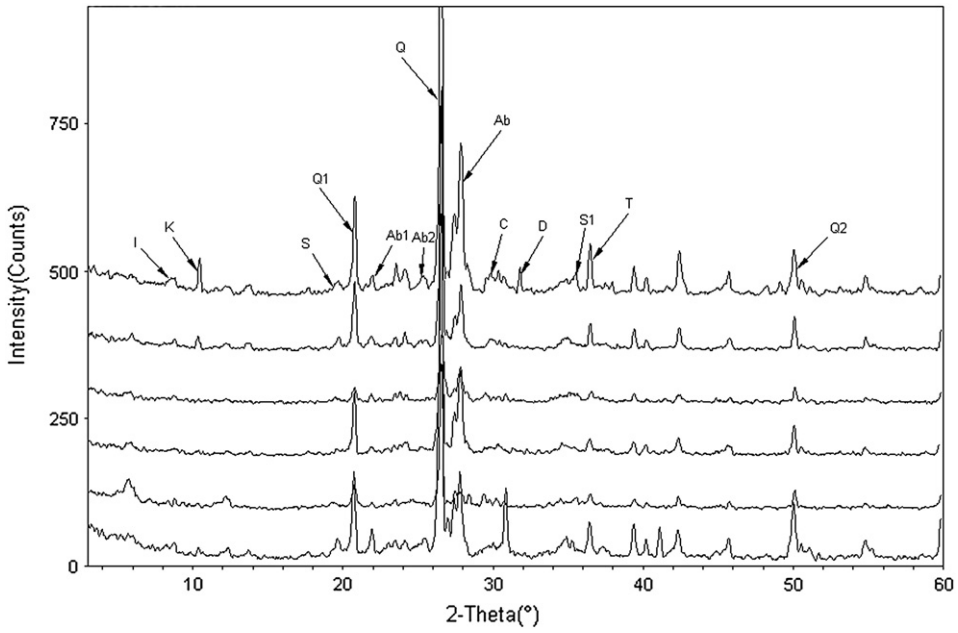

Fig. 2. Mineral composition of selected soils in the study area (Q—quartz, Ab—feldspar, S—montmorillonite, D—dolomite, C—calcite, I—illite, K—kaolinite, T-iron ore).

samples (80% of the samples), the concentrations of Be, Ba, Cr, Ni, Cu, Zn, Cd and Hg are higher than the soil background values in Beijing. (China National Environmental Monitoring Centre, 1990), and their mean values are1.3 times, 1.5times, 1.8 times, 1.6 times, 2 times, 1.2 times, 3 times and 6.3 times of the background value, respectively. In more than 21 of the total 30 samples (70% of the samples), the concentrations of V and Co are higher than the soil background values in Beijing, and their mean values are1.4 times, 1.2 times of the background value, respectively. This result indicates that the iron ore soils have been polluted by trace elements. The maximum concentrations of Cr, Cu, Cd and Hg are 4.2 times, 4.9 times, 4.3 times and 14 times of the soil background values in Beijing, respectively, showing that there is a certain degree of trace element enrichment in soils. Pollution by Hg is most serious. In only about 13% samples, the concentrations of Pb and As are higher than the soil background values in Beijing, and their average values are 0.82 and 0.65 times of the background value in Beijing, respectively. Furthermore, the maximum content of Cr, Co, Ni, Zn, Cd and Hg was detected in the lower reaches of Chao River (such as at sampling point S20), and the minimum was in the upper reaches of Chao River (such as at sampling point S17, S23). Mining and smelting activities in the iron ore area have clearly had a serious influence on the water and soil in the lower reaches of Chao River. Most importantly, the lower reaches of Chao River flow to the Miyun Reservoir, which is the only surface drinking water storage for Beijing residents, so the Chao can seriously affect the quality and safety of drinking water for all the citizens in Beijing.

Among the selected trace elements in the iron mine area soils, Be, V, Co, Cd, Pb, As and Hg manifested almost comparable mean and median concentrations, and exhibited the lowest asymmetry. The remaining trace elements showed that median values were less than their mean concentrations. Large standard deviations (SD) were found in all trace elements levels in all iron mine soil samples (Table 1), which indicated a wide variation of contents in the study area soils. In iron mine area soils, the skewness values of all trace elements were larger than zero. This meant that these elements positively skewed toward low values, in accordance with the fact that their median concentrations were lower than their mean concentrations (Lu et al., 2010). High kurtosis was observed due to the presence of outliers, which corresponded to samples with elevated concentrations of trace elements formic contamination hot spots.

The mean concentrations of Be, Ba, V, Cr, Co, Ni, Cu, Zn, Cd, Pb, As and Hg in size graded soil are shown in Fig. 3. The trend of each trace element concentration increased in smaller particles, fell suddenly to their minimal level in the 50–74 μm size fraction, then increased until reaching a maximum level in the <2 μm colloid size fraction. On the whole, the concentration of trace elements increases with decreasing particle size, and the linear analysis of trace element concentrations and organic matter showed that trace elements and organic matter content were positively correlated (Fig. 4), possibly forming complexes with organic matter. This result is consistent with Table 2.

The results indicate that, the smaller soil particle size is, the more reactivity between the trace elements and organic matter have, and the greater ability to enrich trace elements. Overall, the potential risk caused by the soil fine particles is higher and cannot be ignored.

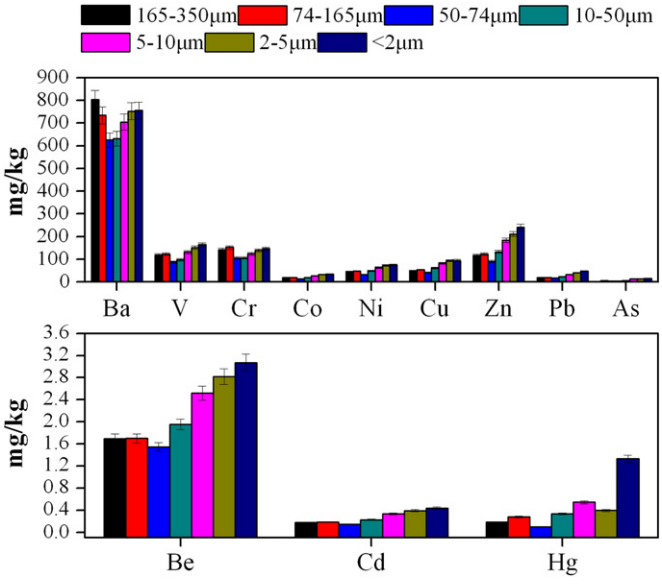

Fig. 3. Mean contents (mg · kg^{-1}) and standard error of selected essential trace elements in seven particle size fractions (μm) (n = 10).

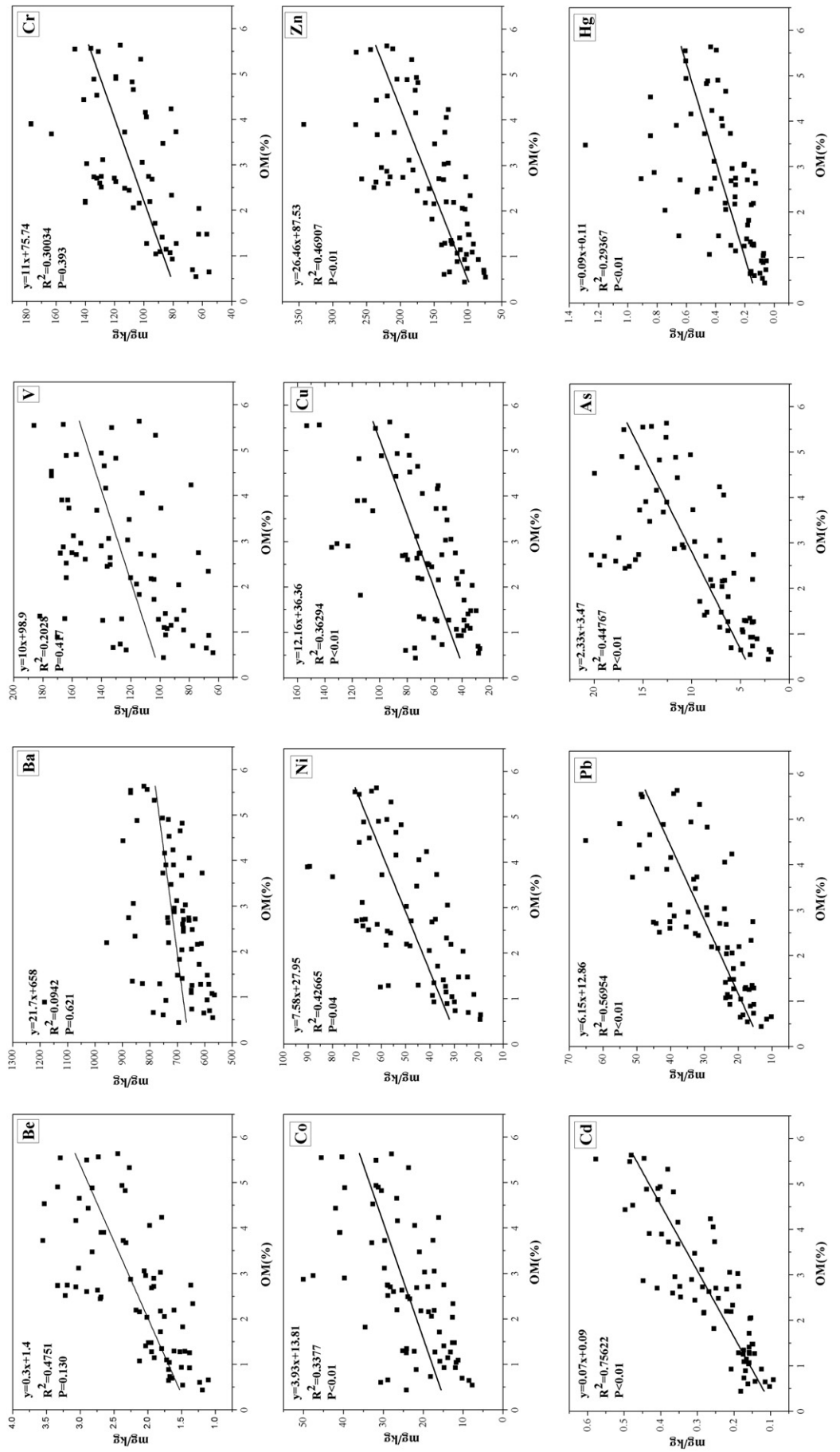

Fig. 4. The correlation analysis between element contents and OM of selected essential samples in particle size fractions (μm).

Table 2
Correlation coefficients for trace elements,organic matter,and pH in soils from iron ore areas along the bank of Chao River.

	Be	Ba	V	Cr	Co	Ni	Cu	Zn	Cd	Pb	As	Hg	pH	OM
Be	1													
Ba	0.172	1												
V	−0.077	0.536**	1											
Cr	−0.740**	0.181	0.515**	1										
Co	−0.610**	0.177	0.680**	0.810**	1									
Ni	−0.765**	−0.072	0.285	0.902**	0.833**	1								
Cu	−0.684**	−0.187	0.201	0.511**	0.715**	0.649**	1							
Zn	−0.384*	0.020	0.228	0.355	0.649**	0.521**	0.775**	1						
Cd	−0.287	−0.036	0.030	0.152	0.299	0.280	0.399*	0.623**	1					
Pb	0.835**	0.028	−0.086	−0.564**	−0.534**	−0.607**	−0.688**	−0.300	−0.048	1				
As	0.683**	−0.322	−0.389*	−0.682**	−0.636**	−0.599**	−0.496**	−0.356	−0.002	0.712**	1			
Hg	−0.242	0.109	0.131	0.287	0.425*	0.417*	0.334	0.375*	0.398*	−0.207	−0.227	1		
pH	0.178	0.145	0.082	−0.129	−0.002	−0.072	−0.076	−0.112	0.168	0.149	−0.499**	−0.301	1	
OM	0.283	−0.094	−0.154	−0.342	−0.342	0.322	−0.329	−0.115	0.310	0.545**	0.575**	0.156	0.465**	1

** Significant *p*-values ($p < 0.01$) (2-tailed).
* Significant *p*-values ($p < 0.05$) (2-tailed).

4. Discussion

4.1. Source identification

4.1.1. Correlation analysis

Correlation analyses can determine the origins of trace elements in soil and the controlling factors of changes in content (Li, 2008). The results of the correlations between trace elements, pH and OM (Table 2) illustrate different origins and behaviors of trace elements in bulk samples.

The coefficients calculated for bulk samples indicated a strong negative correlation between some trace elements and pH and an especially strong negative correlation between As and pH ($p < 0.01$). These indicate that pH is one of the important factors that affect the distribution of trace elements, and the concentration of trace elements is likely to be greater under more acidic conditions.

The strong positive correlations ($p < 0.01$) among Cr, Co, Ni, Cu and Zn shows a similarity in their change rules, and environmental geochemistry of these trace elements in the study site is similar, indicating common pollution sources. This is consistent with the conclusions of Huang et al. (2012) about the soil of Miyun Reservoir's upstream iron mining area. There are strong negative correlations between this group (Cr, Co, Ni, Cu and Zn) and Be, Pb and As, which indicates that the latter have different origins. Furthermore, most of the concentrations do not exceed the soil background values of Beijing, therefore Be, Pb and As are nearly unaffected by anthropogenic sources.

The relationship between each size fraction and the organic matter was examined via linear regressions (Fig. 4): Be: $y = 0.3x + 1.4$, $p = 0.130$; Ba: $y = 21.7x + 658$, $p = 0.621$; V: $y = 10x + 98.9$, $p = 0.417$; Cr: $y = 11x + 75.7$, $p = 0.393$; Co: $y = 3.93x + 13.8$, $p < 0.01$; Ni: $y = 7.58x + 28$, $p = 0.04$; Cu: $y = 12.16x + 36.4$, $p < 0.01$; Zn: $y = 26.46x + 87.5$, $p < 0.01$;Cd: $y = 0.07x + 0.09$, $p < 0.01$; Pb: $y = 6.15x + 12.9$, $p < 0.01$;As: $y = 2.33x + 3.47$, $p < 0.01$; and Hg: $y = 0.09x + 0.11$, $p < 0.01$. There was a positive correlation between trace elements and organic matter and particularly strong relationships for certain trace elements. Co, Cu, Zn, Cd, Pb, As, and Hg were all correlated with *p*-values less than 0.01. The concentrations of Co, Cu, Zn, Cd, Pb, As, and Hg increase with increasing organic matter and are significantly correlated ($p < 0.01$). These trace elements easily formed complexes, chelated and were adsorbed onto organic matter. This conclusion is valuable for managers attempting to control trace element pollution caused by mining, beneficiation and smelting. The relationships between trace elements and organic matter in different size fractions are showed in Table 3. According the relationship between Spearman's rank correlation coefficient and correlation: significant correlation (0.5–1.0 and −1.0 to −0.5), medium correlation (0.3–0.5 and −0.5 to −0.3), low correlation (0.1–0.3 and −0.3 to −0.1) and uncorrelated (0.0–0.09 and −0.09 to 0.0), we can arrive at that almost all the trace elements have significant correlation with organic matter in different size fractions, the result is consistent with the above.

According to Fig. 5, there is also study about the relationship between particle sizes and organic matter content. Different colors represent different particle sizes, their locations explain the relationship between organic matter and trace element in different particle sizes. On the whole, the concentrations of each trace element in the coarse fraction soil were lower than those in fine particle soil, and increase with the decrease of particle size, which indicates that it is easier for fine particle soil to have the adsorption complexing and chelation with trace elements. What is more, we can draw the possible pollution

Table 3
The Spearman's rank correlation coefficient between trace elements and organic matter in different size fractions.

	Be	Ba	V	Cr	Co	Ni	Cu	Zn	Cd	Pb	As	Hg
S1	0.071	0.357	0.428	0.821	0.428	0.286	0.071	0.107	0	0.071	0.428	0.536
S3	0.893	0.536	0.857	-0.143	0.821	0.857	0.964	0.964	1	0.857	0.928	0.857
S10	0.964	0.857	0.928	0.964	0.964	0.964	0.893	0.928	0.893	0.928	0.857	0.75
S12	0.928	0.893	0.964	0.857	0.964	0.857	0.857	0.928	0.964	0.964	0.786	0.357
S13	0.821	0.928	0.964	0.964	1	0.928	0.893	0.857	0.893	0.857	0.928	0.607
S15	0.785	-0.25	0.786	-0.232	0.857	0.786	0.857	0.928	0.786	0.750	0.786	0.786
S22	0.893	0.536	0.25\	0.179	0.75	0.75	0.857	0.893	0.893	0.821	0.893	0.893
S24	0.857	0.143	0.964	0.928	0.964	0.964	0.928	0.964	0.821	0.928	0.786	0.857
S25	0.857	-0.036	0.786	0.678	0.857	0.893	0.964	0.893	0.893	0.893	0.857	0.893
S27	0.964	0.178	0.25	0.178	0.857	0.964	0.964	0.964	0.928	0.928	0.928	0.893

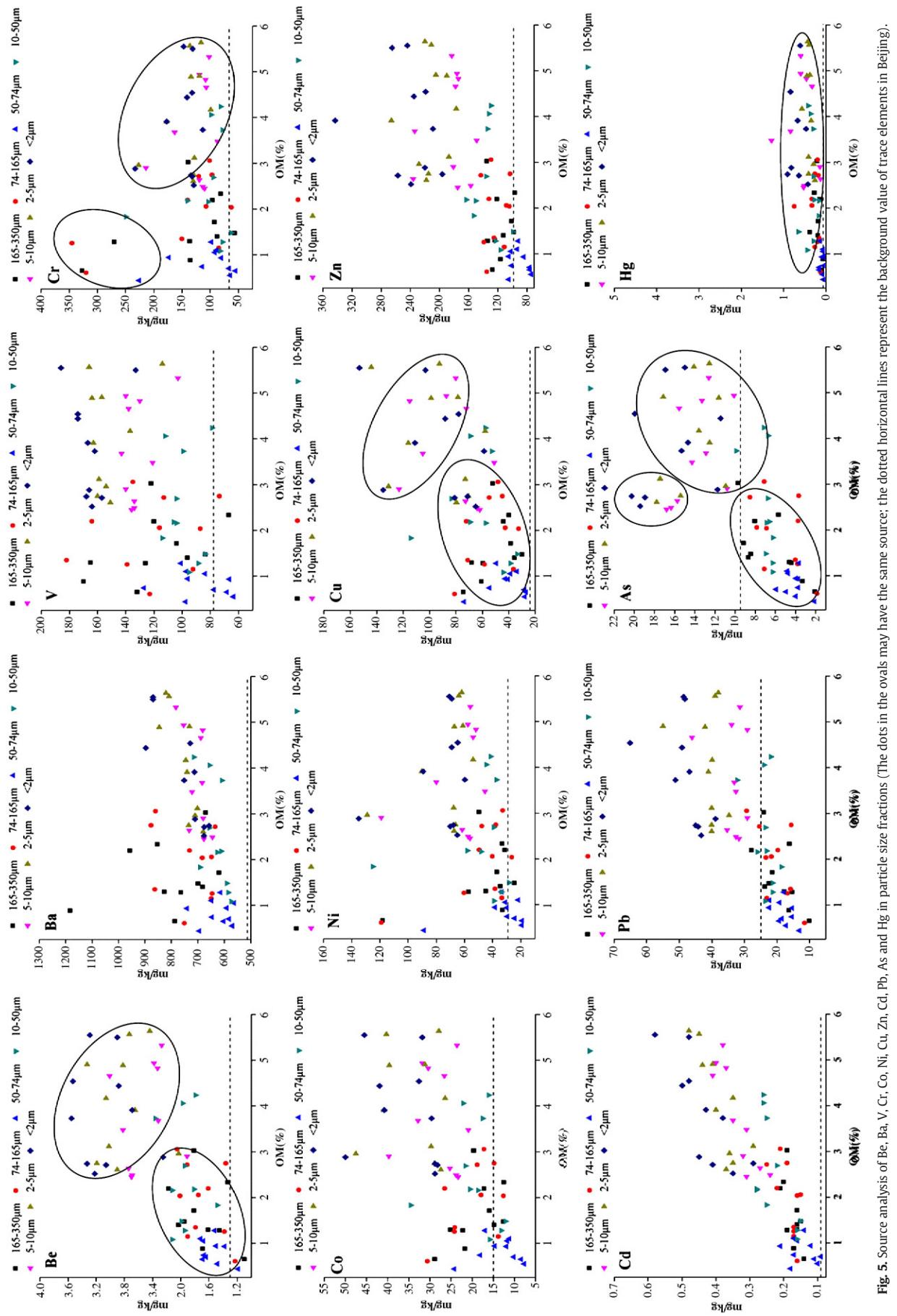

Fig. 5. Source analysis of Be, Ba, V, Cr, Co, Ni, Cu, Zn, Cd, Pb, As and Hg in particle size fractions (The dots in the ovals may have the same source; the dotted horizontal lines represent the background value of trace elements in Beijing).

sources of trace elements by seven different color scattergram, each ellipse stands for different sources of trace elements significantly. In general, the sources of trace elements in coarse fraction soil may be the minerals generated in the process of mining, the sources of trace elements in fine particle soil may be dust deposition and atmospheric precipitation, etc. in mining, mineral smelting and other activities.

The trace element content of these in small particle sizes is high because of fine particle pollution, and fine grains can be transported by winds that determine their final settlement locations, causing the high trace element content in the small particle size material in the area.

4.1.2. Principal component analysis

We used a PCA to identify the sources of pollutants. In order to reveal the origins of trace elements and their intrinsic relations, we analyzed the concentrations of Be, Ba, V, Cr, Co, Ni, Cu, Zn, Cd, Pb, As and Hg from 30 bulk soils and 70 size fractions. The results are shown in Tables 4 and 5. According to the criteria of eigenvalue greater than 1 and cumulative contribution rates greater than 85%, we selected four principal components, which accounted for 90.751% of the total variation. The method of rotation of the component model is varimax with normalization. The eigenvalue of the fourth rotating component is 1.015, which is higher than the original; thus, trace elements can be divided into four components.

Table 5 shows the factor loadings of the principal components. The first component (PC1) explained 40.1% of the total variance and displayed loadings on Be (0.960), V (0.526), Zn (0.760), Cd (0.806), Pb (0.952), and As (0.927), but the factor loadings of V, Zn and Cd were lower than those of Be, Pb and As; therefore, the behavior of elements in this group may be relatively independent. Taking into account that 80% of the concentrations exceeded background values in Beijing, they can be classified as having mixed sources. Be, Pb and As are mainly controlled by rock weathering erosion. In Fig. 6(a), the graphical projection of the PCA results shows that is Zn close to Cd, whereas Be and Pb are close to As. The second component (PC2), which describes 31.9% of the total variance and the loadings on Cr (0.883), Co (0.832), Ni (0.943), and Cu (0.812), reveals an association of strongly correlated elements with a strong positive skew. In Fig. 6 (a and b), the graphical projection of the PCA results shows Cr near Ni and Co close to Cu. Combined with their concentration changes and degree of enrichment, this group appears to be controlled by mixed sources. The third component (PC3) accounts for 10.3% of the total variance and has loadings on Ba (0.970). The result is consistent with Fig. 6(b). The fourth component (PC4), accounts for 8.5% of the total variance and has loadings on Hg (0.920). Because if its high concentration and enrichment degree, this group is highly variable and represents an association among contaminants driven by human activities. The result is consistent with Fig. 6(c).

Table 4
Total variance of trace elements in soils by PCA.

Heavy metals	Component			
	PC1	PC2	PC3	PC4
Be	0.969	−0.135	0.029	−0.010
Ba	0.031	0.079	0.960	0.104
V	0.604	0.481	0.461	−0.137
Cr	−0.137	0.913	0.102	−0.045
Co	0.611	0.754	0.132	0.062
Ni	0.250	0.917	−0.092	0.036
Cu	0.521	0.746	−0.010	0.049
Zn	0.838	0.439	0.004	0.100
Cd	0.869	0.323	0.030	0.172
Pb	0.968	0.000	0.008	0.076
As	0.946	−0.053	−0.129	−0.017
Hg	0.389	0.052	0.113	0.898

4.1.3. Cluster analysis

In order to further reveal the similarity of trace elements, a cluster analysis was carried out on the concentration of trace elements in soil by using SPSS software. The result is shown in a dendrogram (Fig. 7) that groups all of the soil samples into four statistically significant clusters. Be, Pb As, Co, Cu, V, Zn, and Cd form cluster 1. When the distance in the dendrogram is less than 5, cluster 1 can be further divided into four subclusters, namely Be–Pb–As, Co–Cu, Zn–Cd and V, illustrating that the possible pollution sources are different and mainly affected by parent material rock weathering erosion. Hg is alone in cluster 2. It is remarkably different from the other elements in terms of Euclidian distance, which implies a different origin from the other elements, and it is mainly controlled by human activities. Cr and Ni form cluster 3, mainly under the influence of mixed sources. Finally, Ba is alone in cluster 4, which result is in accord with the PCA.

4.1.4. Distribution maps of elements

We also mapped the distributions of elemental concentrations in soils. The impact of the soils is thus assessed by developing an individual pollution map for each element found in bulk samples. The distribution patterns of 12 elements (Be, Ba, V, Cr, Co, Ni, Cu, Zn, Cd, Pb, As and Hg) were prepared using ARCGIS 9.3 software by interpolation method with inverse distance weighted (Zhu et al., 2012). The spatial distribution patterns of trace elements in soils along the bank of Chao River are shown in Fig. 8.

Examining Fig. 8, we observe that elements Pb and As display a typically uniform distribution, differing from the pollution-derived elements. Green represents non-pollution, which may suggest mainly non-anthropogenic sources and show distributions driven the weathering erosion of parent rock material.

The elements Zn, Cd, Co and Cu display quite similar patterns of distribution (Guo et al., 2013), local pollution situation. The changes in their concentrations across the range are bigger, the high-concentration area appears Yaoting iron ore, Anzigou tailings pond and the entrance of Miyun Reservoir, diffuse into the surrounding. There may be two reasons: First, it is mainly influenced by dust, solid waste, mill tailings piled up and acid mine drainage generated by mining, smelting and other activities, and also affected by agricultural activities, including sewage irrigation, pesticides and fertilizers application, etc.; Second, the weathering erosion of parent material rock. This confirms the homology of the Zn, Cd, Co and Cu. Another space distribution feature is that their concentrations are influenced by the monsoon, arising centrally in the pollution sources and spreading, the diffusion scale is big. The main way of diffusion is given priority to atmospheric diffusion (Bilos et al., 2001), wind power and the wind are the main control factors of the spatial distribution of trace elements, thus there is obvious directivity in the spatial distribution characteristics of the four trace elements.

Cr and Ni have similar properties (Luo et al., 2012b; Zhao et al., 2010), the characteristic is that the pollution level from west to east gradually reduces, the more serious pollution appears in the entrance of Miyun Reservoir, which may be caused by the toxic gas containing trace elements generated by mining activities, vehicle emissions and automobile tire wear and dust containing trace elements. Element concentrations increase gradually along the Chao River, reach the maximum in the entrance of Miyun Reservoir. The correlation coefficient of Cr and Ni is very high, perhaps the main cause is usually that Cr and Ni in soil mineral is concomitant, the concentration of Cr and Ni is also affected by common soil minerals, therefore, the space structure and distribution of the two trace elements have a certain similarity. Furthermore, average is less than 1 times more than soil background values in Beijing, which shows metal mining and smelting industry causing, a certain extent, Cr and Ni pollution, but not very serious. Industrial and mining activities, transportation and soil minerals are the common sources of Cr and Ni.

The most pronounced pattern on the map of Hg in soils (Fig. 8) is the visible difference in Hg concentrations from other trace elements, and

Table 5
Factor loadings of trace elements in soils.

Size fraction	Be	Ba	V	Cr	Co	Ni	Cu	Zn	Cd	Pb	As	Hg
165–350 μm												
Mean	1.03	1.03	1.04	1.10	1.03	1.02	1.00	1.03	1.12	0.98	1.12	0.53
Median	1.02	1.02	1.04	1.07	1.01	0.98	1.00	1.00	1.10	0.97	1.12	0.56
Min	0.86	0.96	0.92	0.90	0.87	0.89	0.73	0.87	0.98	0.91	0.82	0.19
Max	1.12	1.12	1.19	1.46	1.14	1.19	1.12	1.15	1.36	1.08	1.36	0.88
SD	0.083	0.051	0.084	0.160	0.087	0.096	0.121	0.084	0.111	0.059	0.170	0.238
Skewness	−0.852	0.227	0.252	1.125	−0.444	0.6	−1.337	−0.35	1.093	0.447	−0.849	0.008
Kurtosis	−0.036	−0.555	−0.699	2.243	−0.412	−0.513	1.929	0.259	1.406	−0.705	0.128	−1.356
74–165 μm												
Mean	1.04	0.95	1.08	1.18	1.08	1.08	1.08	1.09	1.20	1.03	0.96	0.78
Median	1.04	0.95	1.04	1.12	1.03	1.05	1.11	1.06	1.17	1.00	0.99	0.68
Min	0.88	0.81	0.98	0.99	0.98	0.96	0.72	0.93	0.96	0.88	0.76	0.40
Max	1.22	1.08	1.34	1.86	1.22	1.21	1.22	1.23	1.36	1.14	1.19	1.59
SD	0.093	0.079	0.104	0.252	0.089	0.084	0.148	0.086	0.121	0.085	0.128	0.367
Skewness	0.204	−0.134	1.989	2.554	0.429	0.434	−1.821	−0.192	−0.384	−0.324	−0.116	1.225
Kurtosis	1.222	0.014	4.458	7.261	−1.358	−0.86	4.048	0.351	0.31	−0.885	−0.005	1.535
50–74 μm												
Mean	0.95	0.82	0.79	0.86	0.72	0.74	0.83	0.81	0.94	0.95	0.80	0.27
Median	0.90	0.84	0.76	0.81	0.66	0.73	0.86	0.77	0.88	0.86	0.79	0.24
Min	0.82	0.61	0.64	0.76	0.57	0.61	0.53	0.74	0.71	0.76	0.51	0.14
Max	1.18	0.91	0.96	1.06	0.96	0.89	1.11	0.95	1.33	1.47	1.13	0.53
SD	0.125	0.105	0.106	0.097	0.119	0.097	0.154	0.077	0.185	0.235	0.212	0.113
Skewness	0.788	−1.173	0.647	1.001	0.792	0.344	−0.303	1.176	1.051	1.566	0.062	1.502
Kurtosis	−0.539	0.307	−0.221	0.591	0.094	−0.921	1.399	−0.116	0.9	1.717	−0.781	2.77
10–50 μm												
Mean	1.20	0.83	0.91	0.88	1.04	1.10	1.22	1.18	1.46	1.25	1.47	0.94
Median	1.16	0.85	0.95	0.89	1.00	1.07	1.16	1.16	1.39	1.23	1.05	0.75
Min	0.98	0.62	0.56	0.67	0.84	0.93	0.85	1.01	1.10	0.90	0.80	0.53
Max	1.47	0.96	1.13	1.03	1.37	1.26	1.71	1.39	1.87	1.79	3.33	1.49
SD	0.146	0.118	0.160	0.115	0.145	0.110	0.235	0.105	0.248	0.284	0.754	0.330
Skewness	0.528	−1.176	−1.192	−0.571	1.262	0.038	0.619	0.329	0.389	0.612	1.847	0.706
Kurtosis	−0.027	0.364	1.689	−0.651	2.484	−0.838	1.372	0.975	−0.345	−0.26	4.146	−0.946
5–10 μm												
Mean	1.54	0.93	1.22	1.09	1.54	1.51	1.68	1.63	2.18	1.78	2.81	1.56
Median	1.49	0.95	1.22	0.98	1.58	1.53	1.72	1.63	2.25	1.77	2.20	1.23
Min	1.38	0.64	0.70	0.76	1.21	1.20	1.25	1.42	1.44	1.38	1.66	0.42
Max	1.89	1.12	1.52	1.46	1.74	1.81	1.95	1.82	2.48	2.80	5.76	4.00
SD	0.164	0.152	0.258	0.261	0.177	0.226	0.252	0.119	0.304	0.446	1.183	1.085
Skewness	1.216	−0.978	−1.065	0.046	−0.814	−0.278	−0.775	−0.091	−1.778	1.401	1.982	1.42
Kurtosis	1.048	0.349	0.684	−1.736	−0.36	−1.332	−0.734	−0.192	3.734	2.202	4.448	2.014
2–5 μm												
Mean	1.72	0.99	1.41	1.24	1.88	1.74	1.90	1.88	2.52	2.19	2.89	1.13
Median	1.64	1.02	1.37	1.07	1.89	1.80	1.95	1.88	2.49	2.13	2.49	1.01
Min	1.50	0.76	0.90	0.81	1.44	1.30	1.42	1.53	1.97	1.58	1.82	0.87
Max	2.01	1.18	1.79	1.72	2.14	2.09	2.44	2.17	2.91	3.34	5.83	1.67
SD	0.181	0.137	0.274	0.308	0.233	0.299	0.325	0.184	0.271	0.543	1.183	0.248
Skewness	0.653	−0.827	−0.698	0.177	−1.158	−0.407	−0.148	−0.439	−0.754	1.024	1.914	1.209
Kurtosis	−1.061	0.007	−0.022	−1.45	0.38	−1.456	−0.397	0.442	0.832	0.958	4.3	1.238
<2 μm												
Mean	1.88	0.99	1.53	1.32	1.98	1.82	1.90	2.15	2.81	2.56	3.27	3.42
Median	1.78	1.02	1.43	1.09	2.05	1.80	1.98	2.01	2.63	2.52	2.71	2.47
Min	1.73	0.75	1.01	0.83	1.48	1.36	1.27	1.90	2.20	1.75	2.12	1.01
Max	2.23	1.13	1.91	1.80	2.29	2.26	2.59	2.50	3.77	3.74	6.26	8.84
SD	0.161	0.121	0.317	0.350	0.266	0.327	0.395	0.221	0.474	0.626	1.234	2.720
Skewness	1.232	−1.04	−0.405	0.026	−0.984	−0.248	−0.104	0.529	0.831	0.455	1.769	1.496
Kurtosis	1.308	0.225	−1.011	−1.821	−0.033	−1.428	0.029	−1.41	0.361	−0.332	3.577	1.012

there is an obvious high-concentration area at the inflow of the Chao River in the northeast zones of Miyun Reservoir. This may be mainly caused by human activities (residents and industrial and mining activities). Moreover, 95% Hg can be quickly held or fixed after into the soil, so the accumulation of Hg in soil is easy (Korre, 1999).

The correlation, PCA and CA analyses are all consistent with these interpretations. Cu, Co, Zn, Cd, and V forms one cluster (Mokrzycki et al., 2003; Nasiman, 1996), originating from both anthropogenic and natural sources. Be, Pb and As pollution is the lightest, showing less enrichment, which may suggest a mainly non-anthropogenic source and be controlled by weathering erosion of the parent rock. Cr, Ni, and Ba are fine particle pollution. The pollution by Hg is most serious. Its concentration is high, and the potential ecological harm index is also high, which may suggest a mainly anthropogenic source and be affected by ore mining, beneficiation, smelting and other activities, and by the emission of large amounts of acid mine drainage.

4.2. Risk assessment

4.2.1. Accumulation factor and enrichment factor analysis

The accumulation factors (AF) were calculated for the 7 size fractions and are summarized in Table 6. All trace elements in all size

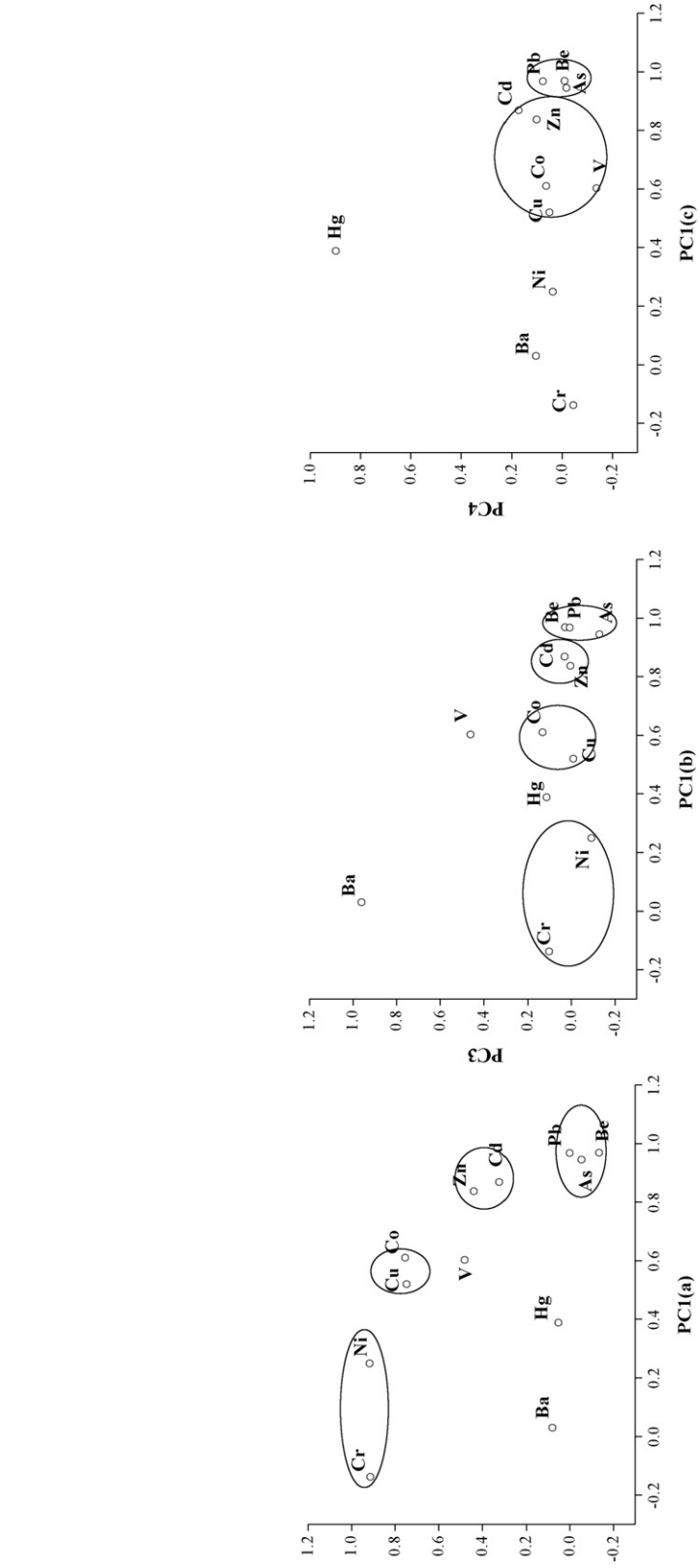

Fig. 6. Loading plots of trace elements in the space defined by two components (The trace elements in the ovals may have the same source).

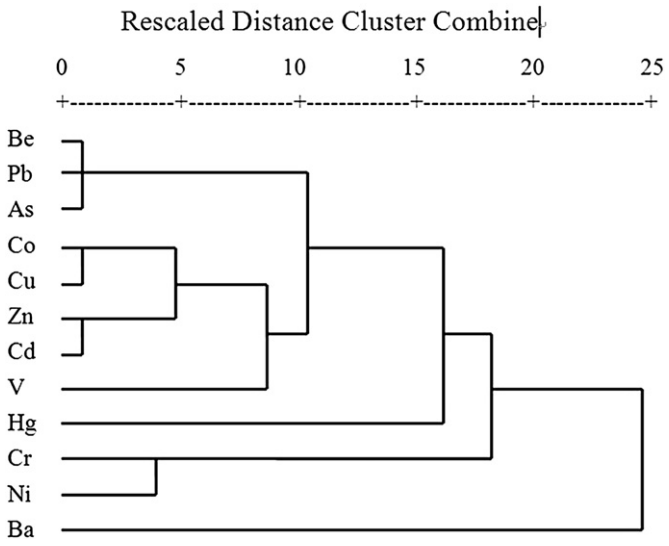

Fig. 7. Hierarchical dendrograms from the hierarchical clustering method (the distances reflect the degree of correlation between different elements) (n = 100).

fractions manifested roughly comparable mean and median concentrations. The mean values of AF in two of the coarse fractions (74–165 μm and165–350 μm), and in the three fine fractions (<2 μm, 2–5 μm and 5–10 μm) are greater than 1. The mean values of AF in < 2 μm, 2–5 μm fine fractions for Cd, Pb, As and Hg are greater than 2, with a maximum of 3.42. In the middle size fractions (10–50 μm, 50–74 μm), the mean values of AF are less than 1.

The higher values of the AF are recorded in 5–10 μm, 2–5 μm and <2 μm fractions for all trace elements, and the highest values are recorded in <2 μm colloid fraction. This indicates that the accumulation in the finer fractions is high. Trace elements accumulate in small particles due to their higher surface area, the negative charges associated with fine particles, the greater availability of clay minerals and their high organic matter, among other factors. The minimum values of the AF are recorded in 10–50 μm and 50–74 μm fractions, indicating that the accumulation is lowest in the two middle fractions. However the accumulation in the coarse fractions (74–165 μm and 165–350 μm) is higher than the middle fractions. The reasons for this mainly include the element additives or iron oxide from industry, organic matter, and aggregation of fine carbonate particles (Barberis et al., 1992). On the whole, the AF values showed a trend of gradual increase from coarse to fine particle size. Low standard deviations (SD) were found in all trace elements, and the standard deviations also showed a trend of gradual increase from coarse to fine particle size, which indicated multiple sources of trace elements in fine particles. The skewness values of the trace elements were larger than zero, which means that their mean values were larger than their median values. Skewness values below zero mean that the mean values are lower than their median values. The skewness values showed a trend of gradual increase from coarse to fine particles. High kurtosis was observed due to the presence of outliers.

Elements selected as a reference element are often conservative, such as the most commonly used elements: Sc, Mn, Ti, Fe, Al, or Ca (Pacyna and Winchester, 1990; Quevauviller et al., 1989). Due to the stable nature of Sc in the process of supergene, we chose it as the standard element to calculate the enrichment factor. Using the latest A-layer soil background values in Beijing as the geochemical background, the concentrations of Be, Ba, V, Cr, Co, Ni, Cu, Zn, Cd, Pb, As, Hg and Sc in the surface soil fraction of each sampling site were standardized for calculation. The results of the enrichment factor (EF) for iron ore areas are shown in Fig. 9.

Fig. 9 shows the enrichment factors of Be, Ba, V, Cr, Co, Ni, Cu, Zn, Cd, Pb, As and Hg in particle size fractions in iron ore areas along the bank of Chao River. In the <2 μm colloid fraction, the trace element enrichment factor (EF) is 8.177 for Hg, implying significant enrichment. Next is Cd, whose EF is 2.875, suggesting moderate enrichment, and a serious influence by anthropogenic factors (Wang et al., 2006). The enrichment factors on the whole gradually increase with decreasing particle size. Trace elements such as Hg and Cd readily react with CO_3^{2-} to form element–carbonate complexes or minerals on the surface of calcitic or dolomitic crystals (Banat et al., 2005). Iron minerals in the <2 μm colloid fraction play a role in trace element enrichment, so the degree of element enrichment in fine particle sizes is higher than in coarse particles. Element enrichment factors (EF) <1.0 were found for Be, Pb and As. The three elements are underenriched and basically uninfluenced by anthropogenic factors, which is consistent with the correlation analysis.

As mentioned above, the concentration of trace elements in fine particles is higher due to their high surface areas, the negative charges associated with fine particles, the greater presence of clay minerals such as smectite and because of the high organic matter content (Acosta et al., 2009). In this study, the high contents of organic matter (2.448%–5.637%) may account for the high levels of trace element accumulations in fine fractions. Meanwhile, silicates accumulate in 5–10 μm, 2–5 μm and <2 μm fine particles containing calcite and dolomite. The larger reactivity of fine particles is caused by the above factors in processes of coprecipitation, absorption, adsorption, and complexation that promote the accumulation of trace elements. Jia and Sun (2001), in a study on characteristics of several types of silicate adsorption of metal ions, found that garnet, pyroxene, quartz and feldspar readily adsorb metal ions (Fe^{3+}, Cu^{2+}, Pb^{2+} and Ca^{2+}) under certain conditions.

4.2.2. Potential ecological risk assessment

In order to reflect the difference within the surrounding area, we chose soil environmental background values of Beijing as the benchmark in this study, and the results are shown in Table 6. The levels of trace element pollution in soils affected by mining, smelting etc. can be seen in Table 6. For the 10 selected soil samples, each sample is divided into seven size fractions. In all 70 size fraction soils, for the <2 μm colloid fraction soils, the RI (≥600) at all 10 sampling points, also implying strong ecological harm. In the 2–5 μm, 5–10 μm and 10–50 μm fine particle soils, 300 ≤ RI < 600 in all 10 sampling points, belongs to the strong ecological harm; in the 50–74 μm, 74–165 μm and 165–350 μm size fraction soils, RI values are below 150 in the 50–74 μm size fraction at 2 sampling points, indicating slight ecological harm, and the remainder all have RI values between 150 and 300 indicating moderate ecological harm.

The E_r^i<40 are recorded in all 10 sampling points for Be, Ba, V, Cr, Co, Ni, Cu, Zn, Pb, and As and for all fractions, indicating only slight

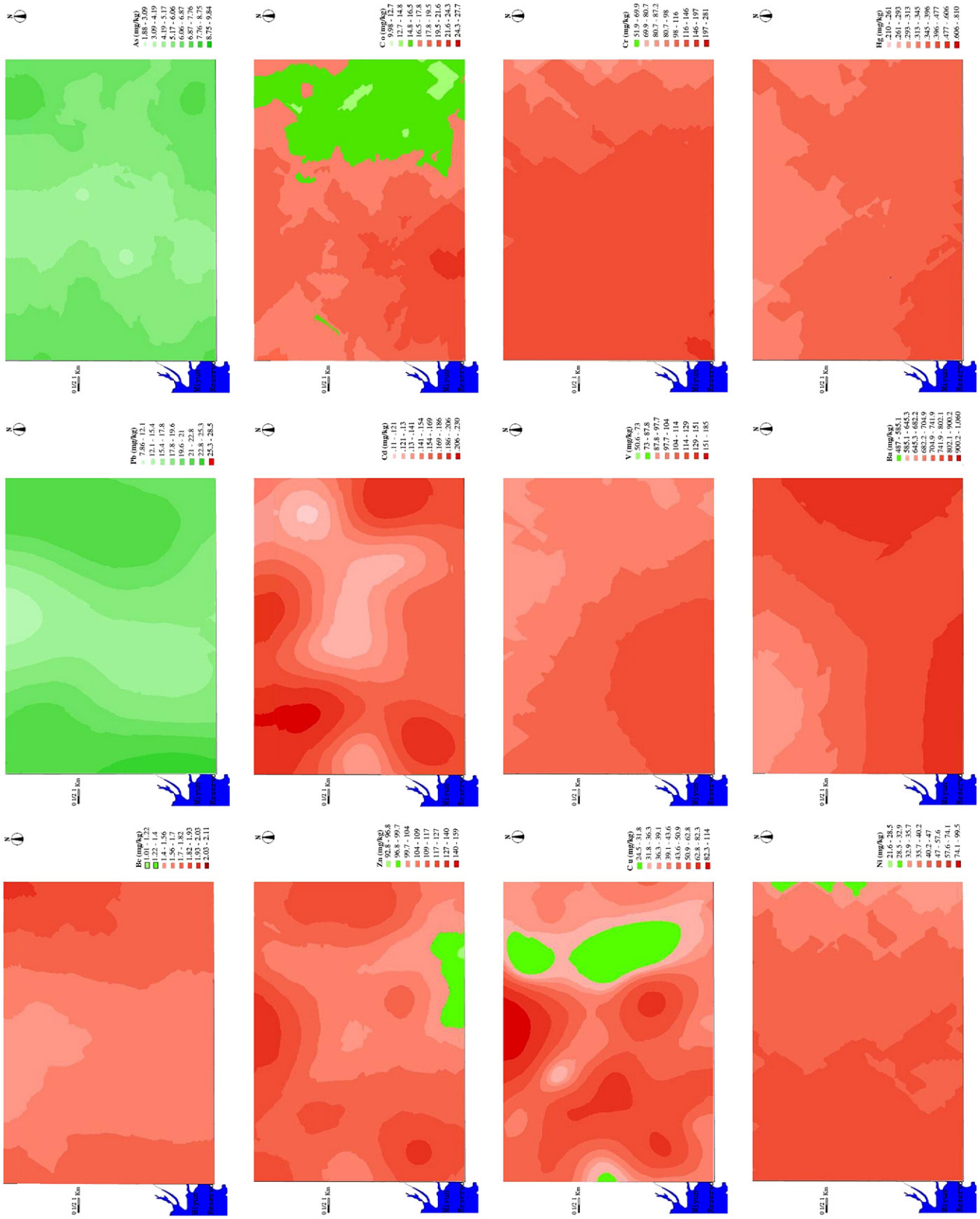

Fig. 8. Distribution maps of concentrations of trace elements in the topsoil.

Table 6
Accumulation factor statistics for each size fraction (n = 10).

Serial number[a]	Size fraction	Be	Ba	V	Cr	Co	Ni	Cu	Zn	Cd	Pb	As	Hg	RI
		(E_r^i)	(E_r^i)	(E_r^i)	(E_r^i)	(E_r^i)	(E_r^i)	(E_r^i)	(E_r^i)	(E_r^i)	(E_r^i)	(E_r^i)	(E_r^i)	
S1	165–350 μm	6.46	4.90	8.52	4.17	6.53	8.79	11.26	1.39	106.2	4.86	10.31	143.06	316.43
	74–165 μm	5.18	5.59	8.80	3.60	6.27	8.44	11.84	1.47	139.9	5.14	9.06	126.39	331.67
	50–74 μm	7.25	4.99	6.73	2.75	3.90	5.48	8.38	1.05	89.33	3.89	5.04	51.39	190.18
	10–50 μm	6.96	5.12	5.83	3.09	6.20	8.53	12.38	1.54	158.4	5.26	7.30	107.64	328.28
	5–10 μm	6.46	4.54	7.27	3.57	8.43	10.92	15.76	2.43	150.6	7.15	16.74	87.50	321.33
	2–5 μm	3.93	5.76	9.22	7.14	9.13	11.95	17.23	2.24	206.2	8.12	18.91	182.73	482.54
	<2 μm	5.75	6.05	11.53	3.96	9.40	12.43	17.53	2.64	229.8	8.95	20.14	445.73	773.89
S3	165–350 μm	4.75	6.24	4.67	8.10	7.40	10.11	12.86	1.38	105.1	3.10	4.69	104.17	272.53
	74–165 μm	7.75	7.00	8.38	10.34	8.07	10.69	12.62	1.43	97.75	3.38	4.03	141.67	313.11
	50–74 μm	6.04	8.66	11.88	5.19	4.90	6.79	9.24	1.08	69.66	4.53	4.20	36.11	168.28
	10–50 μm	6.82	4.64	7.89	4.20	6.83	10.27	14.96	1.68	157.9	4.68	7.01	185.42	412.27
	5–10 μm	4.93	4.73	9.71	4.89	10.93	14.17	22.73	2.41	198.3	6.70	13.72	585.42	878.65
	2–5 μm	6.79	4.75	6.45	9.78	13.63	15.99	25.11	2.74	223.0	8.32	13.33	244.21	574.13
	<2 μm	7.18	5.00	6.08	5.31	13.60	15.83	24.03	3.53	242.1	9.49	15.62	463.23	811.03
S10	165–350 μm	6.25	4.74	8.10	2.62	4.93	6.12	7.71	1.15	88.76	4.80	9.23	129.86	274.27
	74–165 μm	4.39	5.50	8.59	2.54	4.60	5.92	7.86	1.14	92.70	4.68	7.55	182.64	328.11
	50–74 μm	5.75	5.35	11.46	1.93	2.57	3.44	6.02	0.76	57.30	3.48	4.24	54.17	156.47
	10–50 μm	4.86	6.42	5.14	2.33	4.37	5.96	8.33	1.27	88.20	4.31	6.67	204.17	342.03
	5–10 μm	7.32	6.29	9.43	3.30	7.77	9.95	13.42	1.80	171.9	6.42	17.89	365.28	620.78
	2–5 μm	6.39	6.32	12.71	6.60	9.63	11.77	15.26	2.21	194.9	8.12	16.40	281.36	571.71
	<2 μm	6.00	4.13	5.85	3.87	9.60	11.54	14.07	2.46	193.8	8.77	20.65	299.29	580.05
S12	165–350 μm	5.36	4.33	6.71	1.71	4.20	4.36	6.43	1.01	84.27	4.53	8.97	262.50	394.38
	74–165 μm	5.29	4.17	4.45	1.87	4.20	4.68	7.03	1.07	87.64	4.74	7.32	517.36	649.82
	50–74 μm	6.04	4.41	4.77	1.66	2.82	3.40	5.82	0.78	64.04	3.91	5.26	113.19	216.1
	10–50 μm	5.86	4.26	5.41	1.87	4.03	5.00	7.27	1.02	83.15	4.31	7.40	451.39	580.97
	5–10 μm	4.25	5.08	6.81	2.61	6.97	8.05	11.02	1.53	172.5	6.60	15.19	894.44	1135.02
	2–5 μm	5.43	4.49	7.06	5.21	8.80	9.56	12.51	1.82	198.3	8.08	14.47	393.64	669.38
	<2 μm	4.93	5.42	4.65	3.39	9.87	10.59	12.71	2.15	212.4	10.36	16.30	329.17	621.9
S13	165–350 μm	6.14	4.75	6.78	2.76	5.30	6.52	8.31	1.04	88.76	4.33	9.73	125.00	269.42
	74–165 μm	5.96	4.74	8.87	3.21	5.97	7.13	9.22	1.11	85.96	4.39	8.35	229.17	374.08
	50–74 μm	7.57	4.58	7.27	2.00	3.40	4.31	6.10	0.78	51.69	3.74	6.32	108.33	206.09
	10–50 μm	6.46	4.48	7.40	2.46	5.27	6.90	9.52	1.19	88.76	4.78	6.67	306.25	450.14
	5–10 μm	6.93	4.28	6.18	3.39	7.93	10.18	13.85	1.62	135.9	6.60	17.42	362.50	576.84
	2–5 μm	7.11	4.32	5.83	6.78	9.90	12.00	15.78	1.92	161.2	8.12	18.55	283.49	535.04
	<2 μm	7.57	4.19	6.64	4.02	9.60	12.02	15.41	2.02	160.	9.11	21.55	630.60	882.84
S15	165–350 μm	5.29	5.07	7.96	9.81	9.60	20.92	16.10	1.31	79.78	2.04	2.19	66.67	226.74
	74–165 μm	7.04	4.80	7.82	9.60	10.20	21.10	17.53	1.39	90.45	2.33	1.97	93.06	267.29
	50–74 μm	6.39	5.23	5.50	6.78	8.07	15.73	15.97	1.08	101.7	2.65	2.25	43.75	215.09
	10–50 μm	8.43	4.46	6.93	7.47	11.50	22.16	24.68	1.57	142.7	3.77	6.65	120.83	361.15
	5–10 μm	6.93	4.81	7.27	6.42	13.23	21.10	26.62	1.86	177	5.89	11.49	96.53	379.12
	2–5 μm	9.79	5.37	9.36	12.83	15.83	22.87	28.35	2.35	202.8	7.02	11.64	198.96	527.18
	<2 μm	8.29	5.01	9.99	6.99	16.67	23.94	29.22	2.26	251.7	7.87	12.50	568.69	943.12
S22	165–350 μm	9.64	4.96	9.50	4.08	8.37	7.94	14.72	1.28	88.76	3.58	4.88	96.53	254.24
	74–165 μm	10.07	5.28	8.45	4.20	8.83	8.78	15.61	1.36	123.6	3.99	3.97	231.25	425.39
	50–74 μm	9.61	4.72	9.36	2.94	5.67	5.96	10.74	0.95	80.34	3.62	3.89	95.83	233.63
	10–50 μm	6.82	4.98	9.78	2.94	7.37	7.89	14.91	1.36	143.8	4.84	7.13	249.31	461.15
	5–10 μm	8.50	5.52	9.78	3.57	10.60	10.21	18.87	1.81	225.3	6.86	10.76	417.36	729.12
	2–5 μm	8.11	5.73	7.20	7.14	13.20	11.90	21.36	1.95	246.1	8.52	12.37	314.23	657.78
	<2 μm	10.75	5.04	9.64	4.23	13.97	12.23	19.07	2.42	279.2	9.96	12.17	3007.4	3386.09
S24	165–350 μm	8.32	4.99	9.08	2.43	4.17	5.89	8.61	0.99	114.0	3.26	6.04	184.72	352.54
	74–165 μm	10.36	4.98	10.55	2.90	4.93	6.68	9.70	1.06	104.5	3.16	3.91	182.64	345.36
	50–74 μm	9.46	5.42	11.39	2.41	3.97	5.30	8.77	0.87	116.3	3.10	3.99	59.72	230.69
	10–50 μm	11.39	5.38	11.18	2.44	5.37	7.34	12.42	1.33	148.3	4.41	7.59	294.59	511.75
	5–10 μm	10.93	5.46	9.57	3.06	7.87	9.91	17.32	1.88	213.5	6.36	13.42	418.06	717.32
	2–5 μm	10.79	5.14	11.11	6.12	9.30	10.98	20.02	2.26	269.7	7.69	13.36	300.14	666.57
	<2 μm	7.25	5.20	10.76	3.93	10.60	12.23	22.29	2.73	271.9	9.78	18.01	2492.9	2867.62
S25	165–350 μm	10.07	6.19	11.46	2.87	5.73	5.55	9.50	1.24	116.3	5.63	8.55	97.92	281
	74–165 μm	8.71	6.01	7.96	3.03	5.73	5.82	10.39	1.33	118.5	5.93	7.56	140.28	321.29
	50–74 μm	11.89	5.36	10.97	2.67	3.73	3.88	7.34	0.96	96.63	4.51	5.12	49.31	202.37
	10–50 μm	9.75	5.92	11.60	2.34	5.83	6.60	11.41	1.38	141.6	6.52	10.50	207.07	420.49
	5–10 μm	10.93	4.95	10.97	3.21	8.87	9.56	15.63	1.83	228.7	9.33	16.57	229.17	549.67
	2–5 μm	9.61	5.22	11.67	6.42	10.40	10.83	16.97	2.11	228.7	11.13	18.22	266.41	597.64
	<2 μm	11.50	4.96	11.46	3.96	10.87	11.49	16.88	2.25	267.4	13.18	21.22	585.77	960.96
S27	165–350 μm	12.68	5.50	11.32	4.05	7.23	5.85	13.10	1.19	94.38	3.30	3.50	50.69	212.79
	74–165 μm	11.89	4.82	11.74	4.50	8.03	6.79	15.35	1.29	97.19	3.20	4.28	111.81	280.89
	50–74 μm	8.04	5.20	11.60	3.42	6.03	5.25	11.80	1.04	96.63	3.12	3.98	38.89	195
	10–50 μm	10.29	6.57	12.16	2.82	7.20	6.93	18.05	1.40	123.0	4.76	7.18	202.78	403.17
	5–10 μm	10.36	6.37	9.29	3.24	10.13	9.18	24.89	1.79	205.1	5.89	14.13	320.83	621.16
	2–5 μm	12.61	5.34	12.16	6.48	13.43	11.33	31.17	2.17	250.0	7.89	15.00	274.10	641.68
	<2 μm	11.75	6.37	12.99	4.41	15.17	12.54	33.12	2.51	324.2	9.86	15.95	420.97	869.8

[a] Sample numbers as shown in Fig. 1.

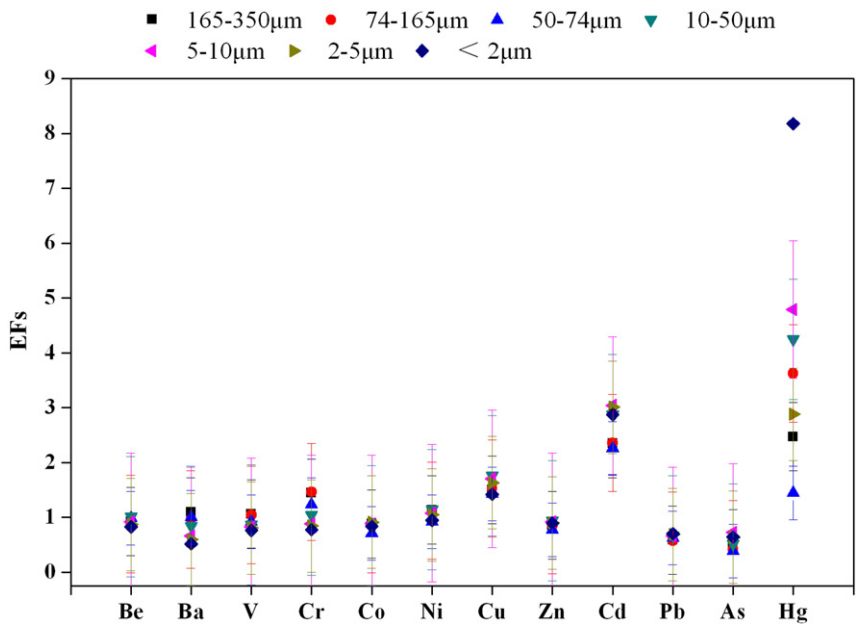

Fig. 9. Mean enrichment factors (EF) of selected essential trace elements in seven particle size fractions (μm) (n = 10).

ecological harm. The degree of pollution for Cd and Hg is higher, causing more serious damage, especially by Hg. This conclusion is consistent with Fig. 8. The main trace element of $E_r^i \geq 320$ is Hg, indicating the greatest ecological harm. The main contributions to the group of greater ecological harm, with $160 \leq E_r^i < 320$, are made by Hg in the 2–5 μm and 5–10 μm size classes and by Cd in the <2 μm, 2–5 μm, and 5–10 μm classes. PM_{10} can remain suspended in the air for a long time, so it can easily enter the human body by hand to mouth contact, inhalation and skin contact (De Miguel et al., 1997). We suggest that the risk assessment of trace elements in mine soils (and elsewhere) should be based on fine particle size because of the tendency of trace elements to accumulate in fine particles.

The results show that the potential ecological risk indices of single element (E_r^i) and various trace elements (RI) increase with decreasing particle size. Because fine fractions have a larger specific surface area, negative charge, high clay content and high organic matter content, trace elements are readily absorbed, coprecipitated, complexed etc. (Tang et al., 2009). This conclusion is consistent with those from the accumulation factor and enrichment factor methods.

5. Conclusions

(1) The concentrations of Be, Ba, Cr, Ni, Cu, Zn, Cd and Hg in the study area are more than 80% above the soil background values in Beijing, and the pollution produced by Hg is most serious. Compared with the above trace elements, Pb and As are less elevated at only 13% beyond the background values. Element pollution in the lower reaches of the Chao River is more serious than the upper reaches, which indicates that mining and smelting activities in the iron ore area have seriously influenced the water and soil in the lower reaches of Chao River.

(2) Correlation and linear analyses show strong negative correlations between some trace elements and pH. The lower the pH is, the higher the concentration of trace elements will be. There was more trace element accumulation with the increase of organic matter. The concentration of trace elements also increased continuously with the increase of soil particle size. Based on PCA and CA analyses, Cu, Co, Zn, Cd and V originate from mixed sources; Be, Pb and As come from natural sources and are mainly affected by the weathering and erosion of parent rock material; Cr, Ni and Ba are the result of fine particle pollution, industrial and mining activities, transportation and soil minerals are the common sources of Cr and Ni; Hg comes from anthropogenic sources, mainly impacted by mining, beneficiation, smelting and acid mine drainage waste.

(3) The EF analysis and potential ecological risk assessment confirm these results. The enrichment factors on the whole gradually increase with decreasing particle size. E_r^i and RI values increase for smaller particles. Hg is the most ecologically harmful and contributes most to the RI, followed by Cd. This conclusion reminds experts to study trace element pollution focusing on fine particles, because the potential ecological harm of fine particles is more serious, and they are more harmful to humans and the environment.

Acknowledgements

We thank Mr. Huang Xingxing for his assistant with field sampling. Furthermore, we are indebted to Prof. Yao Jun and Prof Li Zifu for discussion and suggestions about this study. This work was jointly supported from the National Natural Science Foundation of China (41173113), the International Cooperation Foundation (2012DFA21000) and the Hundred Talents Program of Chinese Academy of Sciences.

References

Acosta, J.A., Cano, A.F., Arocena, J.M., Debela, F., Martínez-Martínez, S., 2009. Distribution of metals in soil particle size fractions and its implication to risk assessment of playgrounds in Murcia City (Spain). Geoderma 149, 101–109.

Adriano, D.C., 1986. Trace Elements in the Terrestrial Environment. Springer-Verlag, New York, Berlin, Heidelberg, Tokyo.

Agbozu, I.E., Ekweozor, I.K.E., Opuene, K., 2007. Survey of heavy metals in the catfish *Synodontis clarias*. Int. J. Environ. Sci. Technol. 4 (1), 93–98.

Ahmed, F., Ishiga, H., 2006. Trace metal concentrations in street dusts of Dhaka City, Bangladesh. Atmos. Environ. 40, 3835–3844.

Ajmone-Marsan, F., Biasioli, M., Kralj, T., Grčman, H., Davidson, C.M., Hursthouse, A.S., et al., 2008. Metals in particle-size fractions of the soils of five European cities. Environ. Pollut. 152, 73–81.

Al, T.A., Blowes, D.W., Martin, C.J., Cabri, L.J., Jambor, J.L., 1997. Aqueous geochemistry and analysis of pyrite surfaces in sulfide-rich mine tailings. Geochim. Cosmochim. Acta 61 (12), 2353–2366.

Ansari, A.A., SinghI, B., Tobschall, H.J., 2000. Importance of geomorphology and sedimentation processes for metal dispersion in sediments and soils of the Ganga Plain: identification of geochemical domains. Chem. Geol. 162, 245–266.

Baek, S.O., Choi, J.S., Hwang, S.M., 1997. A quantitative estimation of source contribution to the concentrations of atmospheric suspended particulate matter in urban, suburban and industrial areas of Korea. Environ. Int. 23, 205–213.

Banat, K.M., Howari, F.M., Al-Hamad, A.A., 2005. Heavy metals in urban soils of central Jordan: should we worry about their environmental risks? Environ. Res. 97, 258–273.
Barberis, E., Ajmone-Marsan, F., Boero, V., Arduino, E., 1992. Aggregation of soil particles by iron oxides in various size fractions of soil B horizons. J. Soil Sci. 42, 535–542.
Bilos, C., Colombo, J.C., SkoruPka, C.N., Rodriguez Presa, M.J., 2001. Source, distribution and variability of airbonre trcae metals in La Plata City aera, Argentina. Environ. Pollut. 111, 149–158.
Brady, N.C., 1985. The Nature and Properties of Soil. Eurasia Publishing House, New Delhi (639 pp.).
Buat-Menard, P., Chesselet, R., 1979. Variable influence of the atmospheric flux on the trace metal chemistry of oceanic suspended matter. Earth Planet. Sci. Lett. 42, 399–411.
Charlesworth, S.M., Lees, J.A., 1999. Particulate-associated heavy metals in the urban environment: their transport from source to deposit, Coventry, UK. Chemosphere 39, 833–848.
Chen, J.Z., Chen, J., Xie, X.J., 2003. Soil pollution and its environmental effects. Soil 35 (4), 298–303.
China National Environmental Monitoring Centre, 1990. Soil Element Background Values of China. China Environmental Science Press, Beijing.
De Miguel, D., Llamas, J., Chacoón, E., Berg, T., Larssen, S., Røyset, O., et al., 1997. Origin and patterns of distribution of trace elements in street dust: unleaded petrol and urban lead. Atmos. Environ. 31, 2733–2740.
Dominici, F., Peng, R.D., Bell, M.L., Pham, L., McDermott, A., Zeger, S.L., et al., 2006. Fine particulate air pollution and hospital admission for cardiovascular and respiratory diseases. J. Am. Med. Inform. Assoc. 295, 1127–1134.
Dong, A., Cnesters, G., Simsimon, G.V., 1984. Metal composition of soil, sediments and urban dust and dirt samples from the Menomone River, Watershed, Wisconsin, U.S.A. Water Air Soil Pollut. 22, 257–274.
Facchinelli, A., Sacchi, E., Mallen, L., 2001. Multivariate statistical and GIS-based approach to identify heavy metal sources in soils. Environ. Pollut. 114 (3), 313–324.
Farnham, I.M., Johannesson, K.H., Singh, A.K., Hodge, V.F., Stetzenbach, K.J., et al., 2003. Factor analytical approaches for evaluating groundwater trace element chemistry data. Anal. Chim. Acta. 490, 123–138.
Förstner, U., Wittmann, G.T.W., 1979. Metal Pollution in Aquatic Environment. Springer-Verlag, New York (486 pp.).
Gao, Y.X., Feng, J.G., Tang, L., Zhu, X.F., Liu, W.Q., Ji, H.B., 2012. Fraction distribution and risk assessment of heavy metals in iron and gold mine soil of Miyun Reservoir upstream. Environ. Sci. 33 (5), 1707–1717.
Government of Canada, 2001. Order adding toxic substances to schedule 1 to the Canadian Environmental Protection Act, 1999. Can. Gaz. 135, 1–8.
Guo, L.Y., Tian, H.S., Peng, H., Li, J., 2013. Environmental geochemical mapping and multivariate geostatistical analysis of heavy metals in topsoils of a closed steel smelter: Capital Iron & Steel Factory, Beijing, China. J. Geochem. Explor. 130, 15–21.
Hakanson, L., 1980. An ecological risk index for aquatic pollution control—a sedimentological approach. Water Res. 14, 975–1001.
Harte, J., Holdren, C., Schneider, R., Shirley, C., 1991. Toxics A to Z, A Guide to Everyday Pollution Hazards. University of California Press, Oxford, England.
Huang, X.X., Zhu, X.F., Tang, L., Ji, H.B., Jin, Y.S., 2012. Studies on the distribution and chemical speciation of heavy metals in the soil of FengJiayu iron mine, Beijing. J. Environ. Sci. 32 (6), 1520–1528.
Ji, H.B., Wang, S.J., Ouyang, Z.Y., Zhang, S., Sun, C.X., Liu, X.M., et al., 2004. Geochemistry of red residua underlying dolomites in karst terrains of Yunnan-Guizhou Plateau I The formation of the Pingba profile. Chem. Geol. 203, 1–27.
Jia, M.X., Sun, C.Y., 2001. Study on adsorption behavior of metal ions on some silicate minerals. Min. Metall. 10 (3), 25–30.
Jordan, G., 2009. Sustainable mineral resources management: from regional mineral resources exploration to spatial contamination risk assessment of mining. Environ. Geol. 58, 153–169.
Kaiser, H.F., 1960. The application of electronic computers to factor analysis. Educ. Psychol. Meas. 20, 141–151.
Korre, A., 1999. Statistical and spatial assessment of soil heavy metal contamination in areas of poorly recorded, complex sources of pollution Part 1: factor analysis for contamination assessment. Stoch. Env. Res. Risk A. 13, 260–287.
Lagerwerff, J.W., Specht, A.W., 1970. Contamination of road side soil and vegetation with cadmium, nickel, lead and zinc. Environ. Sci. Technol. 4, 583–586.
Lee, D.S., Garland, J.A., Fox, A.A., 1994. Atmospheric concentrations of trace metal in urban areas of the United Kingdom. Atmos. Environ. 28, 2691–2713.
Li, Y.H., 1981. Geochemical cycles of elements and human perturbation. Geochim. Cosmochim. Acta 45, 2073–2084.
Li, J., 2008. Analysis and evaluation of heavy metal pollution of the sediment in Xiangjiang river Changzhutan section. Hunan University 21–22.
Li, J.J., Ma, J.T., Chu, X.J., Wang, S.B., Wu, H., Wang, Z.H., 2006. Application of index of geo-accumulation and enrichment factor in safety assessment of heavy-metal contamination in soil of copper refining. China Saf. Sci. J. 16 (12), 135–139.
Li, H.Z., Yang, Z.J., Gu, Z.H., Ma, Z.W., Zhao, J.X., Lv, W.C., et al., 2007. The progression and significance of the study on environmental material renovating the heavy metal ion pollution in the water body. Journal of the Graduates of Sun Yat-Sen University 28 (4), 35–41.
Li, C., Li, F.Y., Zhang, Y., Liu, T.W., Hou, W., 2008. Spatial distribution characteristics of heavy metals in street dust in Shenyang city. Ecol. Environ. 17 (2), 560–564.
Lin, Z.X., Harsbo, K., Ahlgren, M., Qvarfort, U., 1998. The source and fate of Pb in contaminated soils at the urban area of Falun in Central Sweden. Sci. Total Environ. 209, 47–58.
Lin, Y.P., Teng, T.P., Chang, T.K., 2002. Multivariate analysis of soil heavy metal pollution and landscape pattern in Changhua County in Taiwan. Landsc. Urban Plan. 62, 19–35.
Lu, X.W., Wang, L.J., Li, L.Y., Lei, K., Huang, L., Kang, D., 2010. Multivariate statistical analysis of heavy metals in street dust of Baoji, NW China. J. Hazard. Mater. 173, 744–749.
Luo, X.S., Yu, S., Li, X.D., 2012a. The mobility, bioavailability, and human bioaccessibility of trace metals in urban soils of Hong Kong. Appl. Geochem. 27, 995–1004.
Luo, X.S., Yu, S., Zhu, Y.G., Li, X.D., 2012b. Trace metal contamination in urban soils of China. Sci. Total Environ. 421–422, 17–30.
Matini, L., Moutou, J.M., Ongoka, P.R., Tathy, J.P., 2011. Clay mineralogy and vertical distribution of lead, zinc and copper in a soil profile in the vicinity of an abandoned treatment plant. Res. J. Environ. Earth Sci. 3 (2), 114–123 (ISSN: 2041–0492).
Middleton, R., Grant, A., 1990. Heavy metals in the Humber estuary: Scrobienlaria clay preindustrial datum. Proc. Yorks. Geol. Soc. 48, 75–80.
Mokrzycki, E., Uliasz-Bochenczyk, A., Sarna, M., 2003. Use of alternative fuels in the Polish cement industry. Appl. Energy 74, 101–111.
Nasiman, S., 1996. Treatment and reuse of textile wastewater by overlandflow. Desalination 106, 179–182.
Navarroa, M.C., Pérez-Sirvent, C., Martínez-Sánchez, M.J., Vidal, J., Tovar, P.J., Bech, J., 2008. Abandoned mine sites as a source of contamination by heavy metals: A case study in a semi-arid zone. J. Geochem. Explor. 96, 183–193.
Nriagu, J.O., Pacyna, J.M., 1988. Quantitative assessment of worldwide contamination of air, water and soils by trace metals. Nature 333, 134–139.
Nuremberg, H.W., 1984. The voltammetric approach in trace metal chemistry of natural waters and atmospheric precipitation. Anal. Chim. Acta. 164, 1–21.
Oliva, S.R., Espinosa, A.J.F., 2007. Monitoring of heavy metals in topsoils, atmospheric particles and plant leaves to identify possible contamination sources. Microchem. J. 86, 131–139.
Pacyna, J.M., Winchester, J.W., 1990. Contamination of the global environment as observed in the Arctic. Palaeogeogr. Palaeoclimatol. Palaeoecol. 82, 149–157.
Perona, E., Bonilla, I., Mateo, P., 1999. Spatial and temporal changes in water quality in a Spanish river. Sci. Total Environ. 241, 75–90.
Purve, D., 1977. Trace Element Contamination of the Environment. Elsevier, New York 83–115.
Qishlaqi, A., Moore, F., 2007. Statistical analysis of accumulation and sources of heavy metals occurrence in agricultural soils of Khoshk River Banks, Shiraz Iran. Am. Eurasian J. Agric. Environ. Sci. 2, 565–573.
Qu, J., Ma, Z.Y., Cong, Q., Yuan, X., Wang, L.L., 2008. Analysis and assessment on the heavy metals pollution in vegetable soil around the transportation skeleton line in molybdenum ore Areas. J. Agro-Environ. Sci. 27 (1), 178–181.
Quevauviller, P., Lavigne, R., Cortez, L., 1989. Impact of Industrial and mine drainage wastes on the heavy metal distribution in the drainage basin and estuary of the Sado River (Portugal). Environ. Pollut. 59, 267–286.
Rybicka, E.H., 1987. Soil pollution with lead in the region of the domestic glassware plant "Irena" in the Indowroclo Poland. Environ. Technol. Lett. 8, 43–52.
Salman, S.R., Abu Rukah, Y.H., 1999. Multivariate and principal component statistical analysis of contamination in urban and agricultural soils from North Jordan. Environ. Geol. 38, 265–270.
Schulthess, C.P., Huang, C.P., 1990. Adsorption of heavy metals by silicon and aluminum oxide surfaces on clay minerals. Soil Sci. Soc. Am. J. 54, 679–688.
Schultz, L.G., 1964. Quantitative interpretation of mineralogical composition from X-ray chemical data for the Pierre shale. U. S. Geol. Surv. Prof. Pap. 391-C, 31.
Shrestha, S., Kazama, F., 2007. Assessment of surface water quality using multivariate statistical techniques: a case study of the Fuji river basin, Japan. Environ. Model Softw. 22, 464–475.
Sutherland, R.A., 2000. Bed sediment-associated trace metals in an urban stream, Oahu Hawaii. Environ. Geol. 39 (6), 611–627.
Tang, Z.Y., Wu, L.H., Luo, Y.M., 2009. Morphologic analysis and environmental risk assessment of heavy metal elements in sized-fractionation soils. J. Geol. 33 (2), 164–169.
Teng, Y.G., Tuo, X.G., Ni, S.J., Zhang, C.J., 2002. Application of an enrichment factor in determining anthropogenic pollution of heavy metal in topsoil. Soil and Environ. Sci. 11 (1), 13–16.
Tuchschmid, M.P., Dietrich, V., Richner, P., Lienemann, P., Desaules, A., KuE' ndig, R., et al., 1995. Federal Office of Environment, Forests and Landscape (BUWAL). UmweltmaterialienNr, Bern 32.
Usman, A.R.A., Kuzyakov, Y., Stahr, K., 2004. Effect of clay minerals on extractability of heavy metals and sewage sludge mineralization in soil. Chem. Ecol. 20 (2), 1–13.
Vallejo, M., Ruiz, S., Hermosillo, A.G., Borja-Aburto, V.H., Cárdenas, M., 2006. Ambient fine particles modify heart rate variability in young healthy adults. J. Expo. Anal. Environ. Epidemiol. 16, 125–130.
Viklander, M., 1998. Particle size distribution and metal content in street sediments. J. Environ. Eng. 124 (8), 761–766.
Wang, Y.P., Pei, T., Cheng, H.X., Chen, D.X., 2003. Research on the distribution characters of heavy metals in column profile of soil within B City. Bull. Mineral. Petrol. Geochem. 2 (2), 144–148.
Wang, X., Qin, Y., Chen, Y., 2006. Heavy meals in urban roadside soils, part 1: effect of particle size fractions on heavy metals partitioning. Environ. Geol. 50, 1061–1066.
Webster, R., Oliver, M.A., 1990. Statistical Methods in Soil and Land Resource Survey. Oxford University Press, Oxford.
Wenzel, W.W., Jockwer, F., 1999. Accumulation of heavy metals in plants grown on mineralized soils of the Austrian Alps. Environ. Pollut. 104 (1), 145–155.
Xu, Y.N., Zhang, J.H., Zhao, A.N., Ke, H.L., 2008. Evaluation of the potential ecological risk of heavy metals in farmland soils in a certain gold mining area, Xiaoqinling, China. Geol. Bull. China 27 (8), 1272–1278.
Xu, Z.Q., Ni, S.J., Tuo, X.G., Zhang, C.J., 2008. Calculation of heavy metals' toxicity coefficient in the evaluation of potential ecological risk index. Environ. Sci. Technol. 31 (2), 112–115.
Zhao, J., Tang, X., 2011. Distribution of heavy metals in soils with different particle size. Sichuan Environ. 30 (4), 17–20.

Zhao, Y.C., Wang, Z.G., Sun, W.X., Huang, B., Shi, X.Z., Ji, J.F., 2010. Spatial interrelations and multi-scale sources of soil heavy metal variability in a typical urban–rural transition area in Yangtze River Delta region of China. Geoderma 156, 216–227.

Zheng, N., Liu, J.S., Wang, Q.C., Liang, Z.Z., 2010. Health risk assessment of heavy metal exposure to street dust in the zinc smelting district, Northeast of China. Sci. Total Environ. 408, 726–733.

Zhong, X.L., Zhou, S.L., Huang, M.L., Zhao, Q.G., 2009. Chemical form distribution characteristic of soil heavy metals and its influencing factors. Ecol. Environ. 18 (4), 1266–1273.

Zhu, X.F., Ji, H.B., Chen, Y., Qiao, M.M., Tang, L., 2012. Assessment and sources of heavy metals in surface sediments of Miyun Reservoir, Beijing. Environ. Monit. Assess. 2012, 1–14.